DOI: 10.1002/chem.200600144

Synthesis and Structural Model of an α(2,6)-Sialyl-T Glycosylated MUC1 Eicosapeptide under Physiological Conditions

Sebastian Dziadek,[a, c] Christian Griesinger,*[b] Horst Kunz,*[a] and Uwe M. Reinscheid[b, c]

Abstract: To study the effect of O-glycosylation on the conformational propensities of a peptide backbone, a 20-residue peptide (GSTAPPAHGVTSAPDTRPAP) representing the full length tandem repeat sequence of the human mucin MUC1 and its analogue glycosylated with the (2,6)-sialyl-T antigen on Thr11, were prepared and investigated by NMR and molecular modeling. The peptides contain both the GVTSAP sequence, which is an effective substrate for GalNAc transferases, and the PDTRP fragment, a known epitope recognized by several anti-MUC1 monoclonal antibodies. It has been shown that glycosylation of threonine in the GVTSAP sequence is a prerequisite for subsequent glycosylation of the serine at GVTSAP. Furthermore, carbohydrates serve as additional epitopes for MUC1 antibodies. Investigation of the solution structure of the sialyl-T glycoeicosapeptide in a H_2O/D_2O mixture (9:1) under physiological conditions (25 °C and pH 6.5) revealed that the attachment of the saccharide side-chain affects the conformational equilibrium of the peptide backbone near the glycosylated Thr11 residue. For the GVTSA region, an extended, rod-like secondary structure was found by restrained molecular dynamics simulation. The APDTR region formed a turn structure which is more flexibly organized. Taken together, the joined sequence GVTSAPDTR represents the largest structural model of MUC1 derived glycopeptides analyzed so far.

Keywords: antigens · conformation analysis · glycopeptides · solid-phase synthesis

Introduction

Tumor immunotherapy utilizing the remarkable specificity of the human immune system for a selective attack on malignant cells would be a highly attractive approach for the treatment of cancer.[1–3] An essential requirement for the development of a functional antitumor vaccine is to focus the highly specific immune reactions on tumor cells ideally without affecting healthy tissue. It is therefore necessary to identify suitable structural elements that clearly distinguish a tumor cell from a normal cell. Such important cancer-selective structural information is observed in the tumor-associated mucin MUC1 which is a heavily O-glycosylated membrane glycoprotein present at the interface between many epithelia and their extracellular environments.[4–6] The extracellular domain of MUC1 consists of tandem repeats comprising 20 amino acids of the sequence GSTAPPAHGVTSAPDTRPAP containing five O-glycosylation sites. In epithelial tumor cells the expression of MUC1 is drastically increased. This MUC1 over-expression is accompanied by the downregulation of a glucosaminyltransferase (C-2GnT-1) and the concomitant over-expression of different sialyltransferases resulting in the formation of short, prematurely sialylated glycan side-chains such as the sialyl-T_N, α(2,3)-sialyl-T, and α(2,6)-sialyl-T saccharide antigens.[7] Moreover, the incomplete glycosylation in tumor cells is supposed to lead to a changed conformation of the protein backbone[8] and to the exposure of peptide epitopes, which are masked in normal cells. A variety of monoclonal antibodies recognize these epitopes and specifically bind to malignant but not normal epithelial cells. Most antibodies are

[a] Dr. S. Dziadek, Prof. Dr. H. Kunz
Institut für Organische Chemie der Universität Mainz
Duesbergweg 10–14, 55099 Mainz (Germany)
Fax: (+49) 6131-39-24786
E-mail: hokunz@uni-mainz.de

[b] Prof. Dr. C. Griesinger, Dr. U. M. Reinscheid
Max-Planck Institute for Biophysical Chemistry
Am Fassberg 11, 37077 Göttingen (Germany)
Fax: (+49) 551-201-2202
E-mail: cigr@nmr.mpibpc.mpg.de

[c] Dr. S. Dziadek, Dr. U. M. Reinscheid
S. Dziadek and U. M. Reinscheid contributed equally to this work.

Supporting information for this article is available on the WWW under http://www.chemeurj.org/ or from the author: Complete list of ROE values used for the structure calculation of the sialyl-T glycoeicosapeptide **13**.

directed to the immunodominant PDTRPAP motif on the MUC1 tandem repeat.[9] These tumor-associated structure alterations render glycopeptide partial structures from MUC1 valuable target molecules for the generation of immunostimulating antigens.

Immunizations of mice with a vaccine construct consisting of a glycopeptide sequence from the MUC1 tandem repeat carrying a sialyl-T_N side-chain conjugated via a flexible spacer with a specific T_H-cell epitope from ovalbumin lead to the induction of a strong, highly specific humoral immune response against the tumor-associated MUC1 glycopeptide.[10] The isolated antibodies from the mouse sera exclusively recognized a combination of saccharide as well as peptide structural elements as determined by a neutralization experiment.[10] In contrast, neither the unglycosylated MUC1 peptide sequence alone nor the sialyl-T_N saccharide antigen attached to a different peptide chain from MUC4 were capable of binding to and hence neutralizing the antibody. These significant results prompted our interest in investigating the structural propensities of tumor-associated MUC1 glycopeptides, in particular the influence of the O-glycans on the conformation of the peptide chain, under nearly physiological conditions in aqueous solution. We herein propose a valuable structural model of the immunogenically relevant parts of the MUC1 peptide core.

Results and Discussion

Syntheses of MUC1-derived glycopeptides: To allow detailed NMR based structural elucidation, eicosapeptides and glycopeptides representing the full length tandem repeat sequence of the mucin MUC1 were synthesized according to an efficient convergent strategy. In order to be able to study the effect of O-glycosylation on the conformational propensities of the underlying peptide backbone, in addition to the glycoeicosapeptide carrying the complex tumor-associated α(2,6)-sialyl-T antigen the unglycosylated MUC1 eicosapeptide was assembled on a solid support. The glycopeptide structure was accessible by incorporating a pre-formed O-glycosyl amino acid into the sequential glycopeptide synthesis.

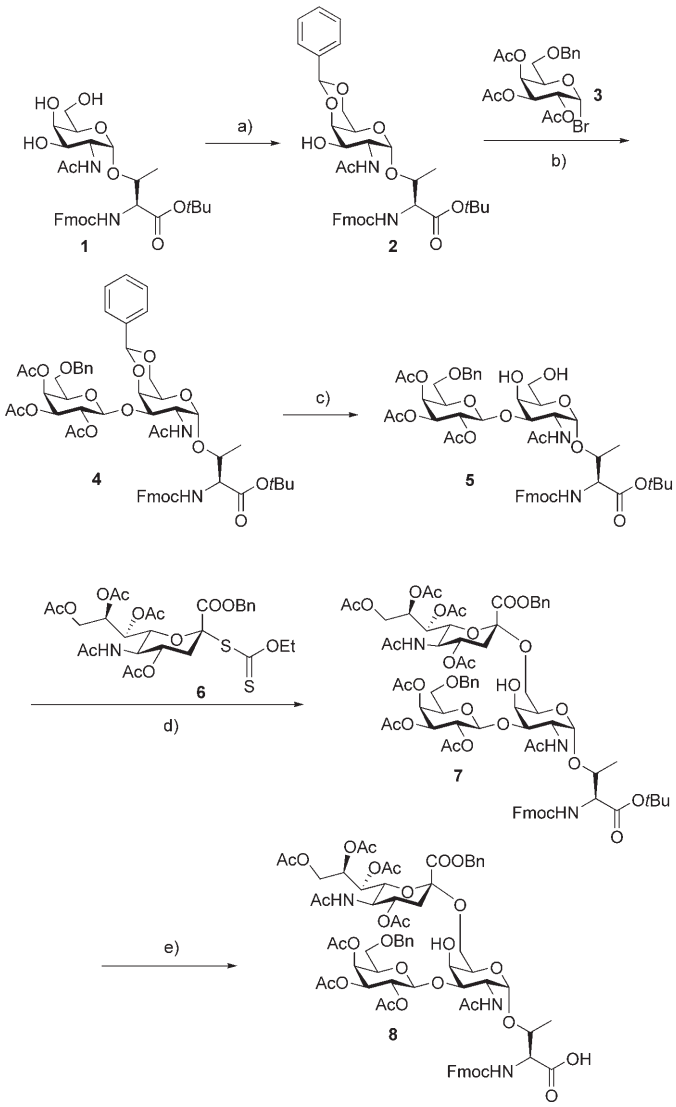

Scheme 1. a) MeCN, α,α-dimethoxytoluene, cat. PTSA, RT, 15 h, 75%. b) $Hg(CN)_2$, CH_3NO_2/CH_2Cl_2 3:2, 4 Å MS, 18 h, 93%. c) 80% AcOH, 80°C, 1 h, 82%. d) MeSBr, AgOTf, 3 Å MS, CH_3CN/CH_2Cl_2 2:1, 4 h, −65°C, 61% α-anomer, 12% β-anomer. e) TFA, anisole, 85%. DTBP = di-*tert*-butylpyridine; PTSA = *p*-toluenesulfonic acid; TFA = trifluoroacetic acid.

Biomimetic synthesis of the O-glycosyl amino acid building block: The preparation of the α(2,6)-sialyl-T threonine building blocks for solid-phase glycopeptide synthesis according to a linear synthetic approach[11] mimicking the glycan biosynthesis in tumor cells is outlined in Scheme 1.

The N-Fmoc and *tert*-butyl ester protected T_N-antigen threonine derivative **1**[12,13] served as synthon for the assembly of the (2,6)-sialyl-T-antigen. It was converted to the 4,6-benzylidene acetal **2** using α,α-dimethoxytoluene in the presence of catalytic *p*-toluenesulfonic acid in acetonitrile. The subsequent stereoselective β-galactosylation to form the blocked disaccharide **4**[11] was accomplished employing the 6-*O*-benzyl protected galactosyl bromide **3**[14] activated with mercury(II) cyanide under Helferich[15] conditions. Selective removal of the benzylidene acetal with aqueous acetic acid at 80°C furnished a suitable sialyl acceptor **5**. For the regio- and stereoselective sialylation of the 6-OH group in **5**, the xanthate[16,17] **6** of the *N*-acetyl neuraminic acid benzyl ester activated with methylsulfenyl triflate[18] as a promoter proved to be an efficient donor. Using a mixture of acetonitrile[19] and dichloromethane for the glycosylation reaction, the desired α(2,6)-sialyl-T-threonine derivative **7** was obtained in a yield of 61% after preparative RP-HPLC. Subsequent acidolysis of the *tert*-butyl ester with trifluoroacetic acid and anisole (10:1) yielded the N-Fmoc protected (2,6)-sialyl-T-threonine building block **8** which was incorporated into the sequential solid-phase synthesis without O-acetylation of the sterically hindered 4-OH group.

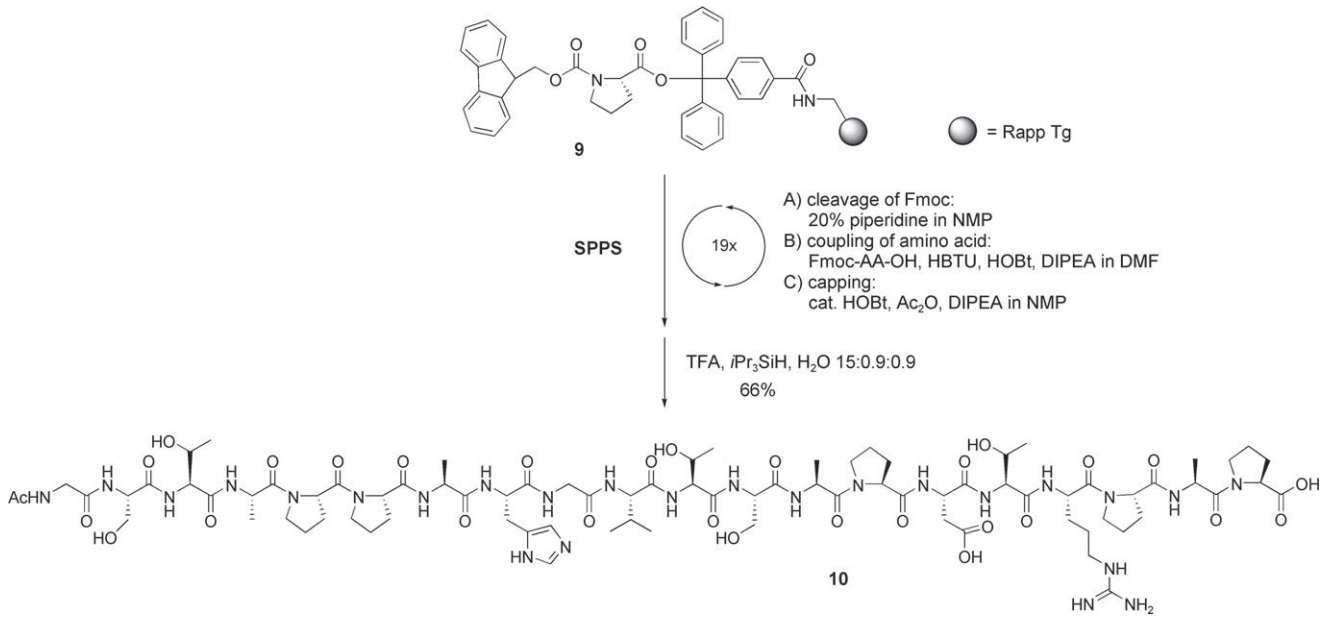

Scheme 2. Solid-phase peptide synthesis of MUC1 eicosapeptide **10**.

Solid-phase glycopeptide synthesis: Prior to the synthesis of different glycoeicosapeptides, the unglycosylated full length tandem repeat sequence of MUC1 was assembled by condensing N-Fmoc[20] and side-chain protected amino acids (10 equiv) on Tentagel resin[21] **9** functionalized with Fmoc-proline via the trityl linker (Scheme 2).

Couplings were achieved by activating the amino acid building blocks with *O*-(1*H*-benzotriazol-1-yl)-*N*,*N*,*N*′,*N*′-tetramethyluronium hexafluorophosphate (HBTU)[22]/*N*-hydroxybenzotriazole (HOBt)[23] and DIPEA. Following each coupling step, unreacted amino components were capped with acetic anhydride/HOBt and DIPEA. After completion of the MUC1 consensus sequence and acetylation of the amino terminus, the peptide was liberated from the resin by acidolysis of the trityl linker under simultaneous removal of all acid-labile side-chain protecting groups. Purification by preparative HPLC and subsequent lyophilization furnished the target structure **10** in a yield of 66%.

To generate suitable model structures for conformational analyses, the threonine residue at position-11, that is, outside the immunodominant PDTRP domain, was chosen for the attachment of the tumor-associated saccharide side chains. For this purpose, the protected resin-bound nonapeptide **11** representing the C-terminal segment of the MUC1 tandem repeat was prepared according to the Fmoc protocol[20] (Scheme 3).

For the synthesis of the (2,6)-sialyl-T glycoeicosapeptide one part of the functionalized resin **11** was employed, which was liberated from the Fmoc group by treatment with piperidine (20%) in NMP. Subsequently, the glycosylated threonine derivative **8** (Scheme 1) was coupled manually to the resin-bound peptide fragment employing an excess of only 1.7 equivalents of the precious building block activated with a combination of the coupling reagents *O*-(7-azabenzotriazole-1-yl)-*N*,*N*,*N*′,*N*′-tetramethyluronium hexafluorophosphate (HATU) and *N*-hydroxy-7-azabenzotriazole (HOAt).[24] Following the coupling reaction and capping of unreacted amino groups, the MUC1 sequence was completed by standard condensations of Fmoc-amino acids and final acetylation of the amino terminus. Simultaneous detachment of the glycopeptide from the polymeric support and cleavage of the acid-labile amino acid side-chain protecting groups was achieved by treatment with a mixture of trifluoroacetic acid, triisopropylsilane and water. The resulting partially deblocked MUC1 glycopeptide **12** was purified by preparative RP-HPLC and isolated in a yield of 44% based on the proline loaded resin **9a**. Final deprotection of the glycan portion by hydrogenolysis of the benzyl groups and O-deacetylation under Zemplén[25] conditions furnished the target structure **13** which was obtained in 55% yield after purification by RP-HPLC.

NMR analysis of the eicosapeptide from MUC1 and its glycosylated analogue: A number of NMR studies have been undertaken to elucidate the structural effects of glycosylation on peptides in general and on MUC1-derived peptides in particular.[8,26] The drawback of "insufficient structure" under physiological conditions was circumvented by lowering the temperature, and/or addition of solvents and adjustment of pH to low values.[27–31] As an example, Kirnarsky et al.[32,33] studied glycosylated 15-mers of MUC1 at low temperatures (5 and 10°C) in water, and 9-mers in DMSO.

We were able to study structural effects of complex carbohydrates on MUC1 derived peptides consisting of the full length tandem repeat in a phosphate buffer of pH 6.5 at 25°C. Using NMR restrained molecular dynamics structured areas could be derived of a full length repeat substituted by complex carbohydrates under physiological conditions. Con-

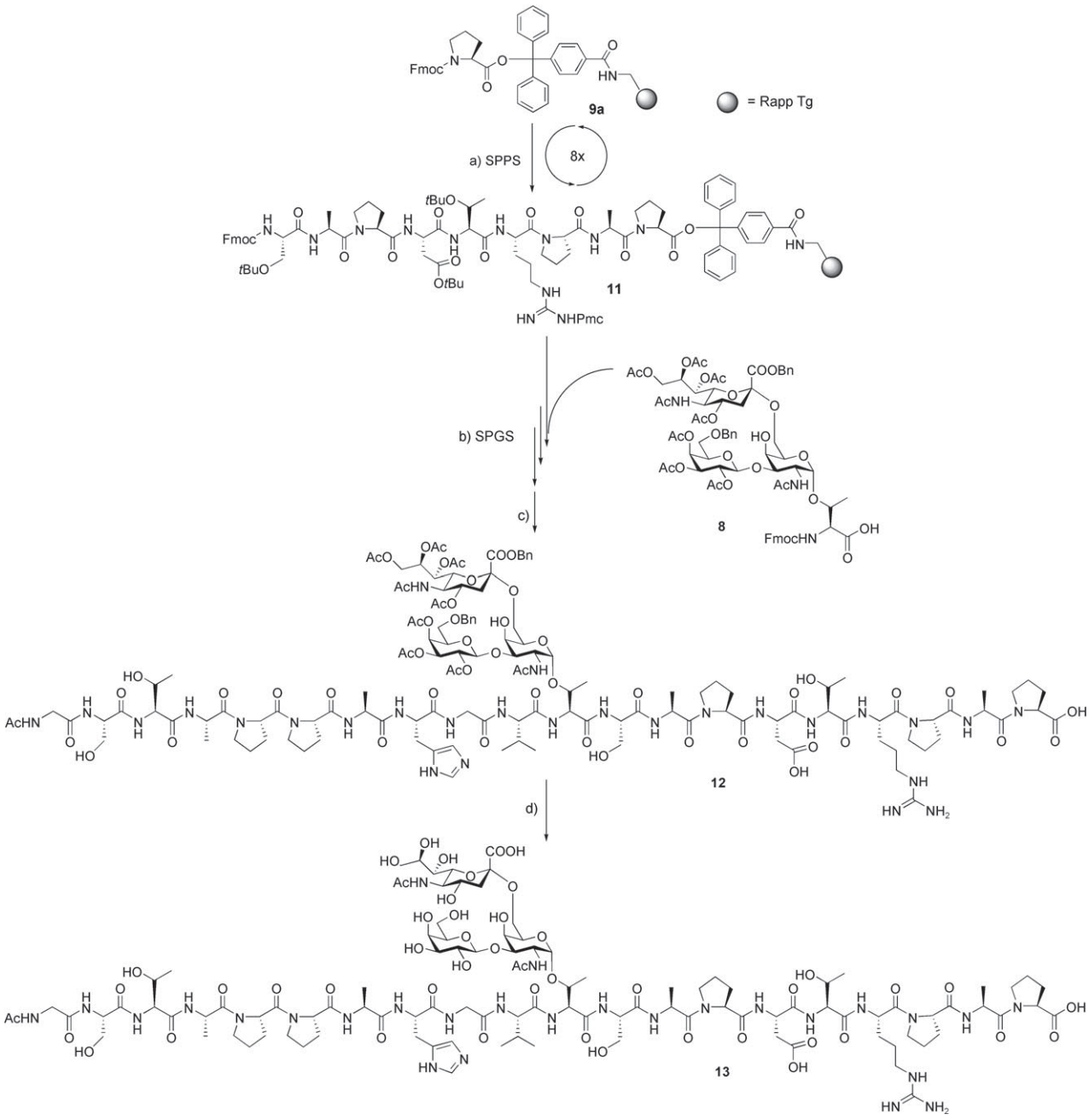

Scheme 3. a) Solid-phase peptide synthesis (SPPS): Fmoc removal (20% piperidine/NMP); coupling (steps 1–8: 1 mmol Fmoc-AA-OH, HBTU/HOBt/DIPEA, DMF; capping: Ac_2O, DIPEA, HOBt 4:1:0.12. Synthesis of (2,6)-sialyl-T glycoeicosapeptide **13** from MUC1: b) solid-phase glycopeptide synthesis (SPGS): Fmoc removal (20% piperidine/NMP); coupling step 9: 1.7 equiv **8**, HATU/HOAt/NMM, DMF, 4 h; steps 10–19: 1 mmol Fmoc-AA-OH, HBTU/HOBt/DIPEA, DMF; capping: Ac_2O, DIPEA, HOBt 4:1:0.12; c) TFA/TIS/H_2O 15:0.9:0.9, 2 h, 44% based on the pre-loaded resin **9a**); d) i) H_2, 5% Pd/C, MeOH, 20 h, ii) NaOMe/methanol, pH 9.5, 55% over two steps. HATU = *O*-(7-aza-benzotriazole-1-yl)-*N*,*N*,*N*′,*N*′-tetramethyluronium hexafluorophosphate, HBTU = *O*-(1*H*-benzotriazol-1-yl)-*N*,*N*,*N*′,*N*′-tetramethyluronium hexafluorophosphate, HOAt = *N*-hydroxy-7-azabenzotriazole, HOBt = *N*-hydroxybenzotriazole; NMM = *N*-methylmorpholine; TIS = triisopropylsilane; Pmc = 2,2,5,7,8-pentamethylchroman-6-sulfonyl.

sequently, direct comparisons with earlier results[8,26–34] have to be treated cautiously.

Proton and ^{13}C NMR resonances were assigned for two MUC1 derived peptides: the unglycosylated full length tandem repeat sequence **10** and the glycosylated peptide **13** (Tables 1–3).

One-dimensional proton NMR spectra showed one predominant resonance for each amide NH suggesting either one dominant isomer or fast conformational averaging on the NMR time scale in phosphate buffer. The coexistence of slowly interconverting conformers could be ruled out by the absence of exchange cross peaks in the ROESY spectra and

Table 1. Chemical shifts (in ppm) of the MUC1 peptide **10** in H_2O/D_2O (9:1, pH 6.5) at 298 K.[a]

	NH	Hα	Cα	Hβ	Cβ	Hγ	Cγ	Hδ	Cδ
G1	8.212	3.893	42.45	–	–	–	–	–	–
S2	8.276	4.457	55.50	a: 3.78, b: 3.818	61.12	–	–	–	–
T3	8.143	4.270	58.83	4.155	67.07	1.114	18.74	–	–
A4	8.148	4.51	47.82	1.249	15.36	–	–	–	–
P5	–	4.61	58.72	a: 2.263, b: 1.794	27.98	1.948	24.7	a: 3.742, b: 3.528	47.6
P6	–	4.291	nd	a: 2.18, b: 1.762	29.28	1.931	24.6	a: 3.724, b: 3.578	47.5
A7	8.316	4.15	49.7	1.241	16.4	–	–	–	–
H8	8.384	4.615	nd	a: 3.207, b: 3.11	26.34	H4: 7.228	C4: 117.425	H2: 8.516	C2: 133.67
G9	8.347	a: 3.871, b: 3.915	nd	–	–	–	–	–	–
V10	8.056	4.140	59.57	2.02	30.18	a: 0.862, b: 0.852	a: 18.39, b: 17.61	–	–
T11	8.245	4.327	58.97	4.137	67.07	1.116	18.74	–	–
S12	8.219	4.371	55.32	a: 3.75, b: 3.891	61.25	–	–	–	–
A13	8.268	4.521	47.85	1.281	15.38	–	–	–	–
P14	–	4.323	nd	a: 2.19, b: 1.829	29.29	1.945	24.5	a: 3.716, b: 3.525	nd
D15	8.505	4.64	50.33	a: 2.874, b: 2.792	35.19	–	–	–	–
T16	7.965	4.236	58.99	4.132	67.07	1.095	18.83	–	–
R17	8.174	4.558	51.19	a: 1.76, b: 1.66	27.46	1.58	23.98	3.127	40.611
P18	–	4.325	nd	a: 2.19, b: 1.796	29.28	1.93	24.5	a: 3.728, b: 3.525	nd
A19	8.326	4.481	47.65	1.284	15.16	–	–	–	–
P20	–	4.305	nd	a: 2.22, b: 1.92	28.88	1.945	24.5	a: 3.693, b: 3.580	nd

[a] nd: not determined.

Table 2. Chemical shifts (in ppm) of the (2,6)-sialyl-T glycoeicosapeptide **13** in H_2O/D_2O (9:1, pH 6.5) at 298 K.

	NH	^{15}N	Hα	Cα	Hβ	Cβ	Hγ	Cγ	Hδ	Cδ
G1	8.216	114.16	3.890	42.52	–	–	–	–	–	–
S2	8.280	115.37	4.454	55.49	a: 3.816, b: 3.777	61.04	–	–	–	–
T3	8.149	115.73	4.267	58.87	4.144	66.95	1.110	18.65	–	–
A4	8.152	127.99	4.505	47.68	1.248	15.21	–	–		
P5	–	–	4.607	58.57	a: 2.260, b: 1.795	27.82	1.944	24.50	a: 3.732, b: 3.527	47.8
P6	–	–	4.290	60.05	a: 2.178, b: 1.754	29.11	1.920	24.50	a: 3.724, b: 3.532	47.6
A7	8.316	124.35	4.142	48.20	1.242	16.28	–	–	–	–
H8	8.328	117.14	4.588	52.49	a: 3.187, b: 3.100	26.59	H4: 7.186	117.63	H2: 8.38	134.15
G9	8.328	120.09	a: 3.838, b: 3.912	43.05	–	–	–	–	–	–
V10	8.016	120.03	4.244	59.28	2.006	30.13	a: 0.890, b: 0.870	a: 18.42, b: 17.67	–	–
T11*	8.660	117.02	4.562	57.11	4.216	77.44	1.216	18.27	–	–
S12	8.450	116.23	4.387	54.96	a: 3.760, b: 3.685	61.50	–	–	–	–
A13	8.432	126.18	4.367	47.75	1.300	14.96	–	–	–	–
P14		–	4.310	60.20	a: 2.215, b: 1.835	29.19	1.958	24.50	a: 3.722, b: 3.556	47.7
D15	8.383	110.10	4.517	51.40	a: 2.64, b: 2.567	38.08	–	–	–	–
T16	7.948	114.16	4.230	58.88	4.143	66.95	1.095	18.70	–	–
R17	8.184	124.69	4.524	51.38	a: 1.751, b: 1.676	29.11	1.594	23.81	3.125	40.56
P18	–	–	4.314	60.30	a: 2.186, b: 1.808	29.22	1.908	24.49	a: 3.730, b: 3.528	47.6
A19	8.240	126.12	4.483	47.46	1.284	15.13	–	–	–	–
P20	–	–	4.136	61.89	a: 2.124, b: 1.810	29.19	1.890	24.39	a: 3.653, b: 3.543	47.4

Table 3. Chemical shifts (in ppm) of the (2,6)-sialyl-T glycoeicosapeptide **13** in H_2O/D_2O (9:1, pH 6.5) at 298 K.

GalNAc				Gal				NeuNAc			
H1:	4.860	C1:	99.31	H1′:	4.325	C1′:	104.70	$H3_{eq}''$:	2.580	C3″:	40.15
H2:	4.125	C2:	48.26	H2′:	3.408	C2′:	70.65	$H3_{ax}''$:	1.543		
H3:	3.900	C3:	77.16	H3′:	3.495	C3′:	72.63	H4″:	3.564	C4″:	68.26
H4:	4.095	C4:	68.99	H4′:	3.800	C4′:	68.64	H5″:	3.727	C5″:	51.85
H5:	4.007	C5:	69.63	H5′:	3.530	C5′:	74.91	H6″:	3.600	C6″:	72.49
H6a:	3.830	C6:	63.85	H6a′:	3.675	C6′:	61.05	H7″:	3.790	C7″:	71.77
H6b:	3.478			H6b′:	3.627			H8″:	3.484	C8″:	68.26
NH:	7.445	^{15}N:	121.68					H9a″:	3.777	C9″	62.65
AcNH:	1.917	C_{Ac}:	22.03					H9b″:	3.550		
								NH:	7.954	^{15}N:	123.04
								AcNH:	1.935	C_{Ac}:	21.90

the correct number of resonances in the 1D proton spectrum. The presence of strong $H_\alpha(i)$–NH(i+1) ROE signals and the absence of $H_\alpha(i)$–$H_\alpha(i+1)$ cross peaks confirmed that all amide bonds were in the *trans* configuration. A *trans* configuration with respect to the X-Pro peptide bonds was indicated by characteristic ROE cross peaks from the H_α (X) to the H_δ (Pro), the absence of cross peaks from H_α (X) to H_α (Pro) and a chemical shift difference of around 31 ppm between C_α and C_β.[35] Additionally, the differences in ^{13}C chemical shifts of C_β–C_γ were around 4.5 ppm which indicated *trans*-peptide bonds.[36,37]

In contrast, Schuman et al.[28] observed two sets of resonances in a MUC1 derived 9-mer suggesting that *cis*/*trans* isomerization occurred at one of the X-Pro peptide bonds. A population ratio of 5:1 was inferred under the experimental conditions (5 °C, pH 5.1). The low signal to noise ratio of the *cis* isomer precluded further structural analysis. In contrast to our results, glycosylation of the 9-mer shifted the *cis*/*trans* equilibrium toward the *trans* isomer for residues at the C-terminal side of the glycosylation. These differing observations might be correlated to different experimental conditions concerning the peptide (sequence, length), the carbohydrates (type, complexity) and the environmental parameters (temperature, pH, solvent system).

A number of side-chain methylene proton pairs exhibited a spectral dispersion that indicated conformational preferences even in the unglycosylated MUC1 peptide. The H_β protons of Ser12 in the unglycosylated peptide **10** showed a $\Delta\delta$ value of 0.15 ppm indicating a non-averaged conformation of the χ_1 dihedral. Upon glycosylation, large chemical shift dispersion was measured within the pair of NH protons of the two Thr residues Thr11 and Thr16, the first of them being glycosylated in **13**. In this glycopeptide the difference increased to more than 0.7 ppm. Conversely, Grinstead et al.[38] observed for a MUC1 hexadecapeptide degenerate H_β resonances of Ser which changed into well resolved peaks only after glycosylation. Again, the experimental conditions may explain these differences.

Chemical shift deviation: Generally, H_α chemical shift deviations (CSD, $\Delta\delta_{H\alpha \text{ or } C\alpha} = \delta_{observed} - \delta_{random\ coil}$) exhibit a mean shift of −0.39 ppm when the residue is placed in a helical conformation while a mean shift of +0.37 ppm is observed when the residue is found in an extended conformation.[35,39] The CSD values, δH_α and δC_α, for the unglycosylated MUC1 derived 20-mer peptide **10** were close to random coil ($\Delta\delta_{H\alpha} \pm 0.02$ ppm and $\Delta\delta_{C\alpha} \pm 0.4$ ppm) for all residues except Ala4 and Pro5 at the N-terminus, and Ala13, Arg17 and Ala19 at the C-terminus. In addition, the H_α resonances for residues near the site of glycosylation in the glycosylated peptide **13** (Figure 1) showed significant downfield shifts for Val10 and Thr11 (+0.104 and +0.235 ppm) whereas Ala13 and Asp15 H_α resonances were shifted upfield by −0.154 and −0.123 ppm, respectively. This is in agreement with an increase in the population of extended structures in the GVTSA region and an ordering effect of the glycan for the PDTR region. The influence of the position of glycosylation

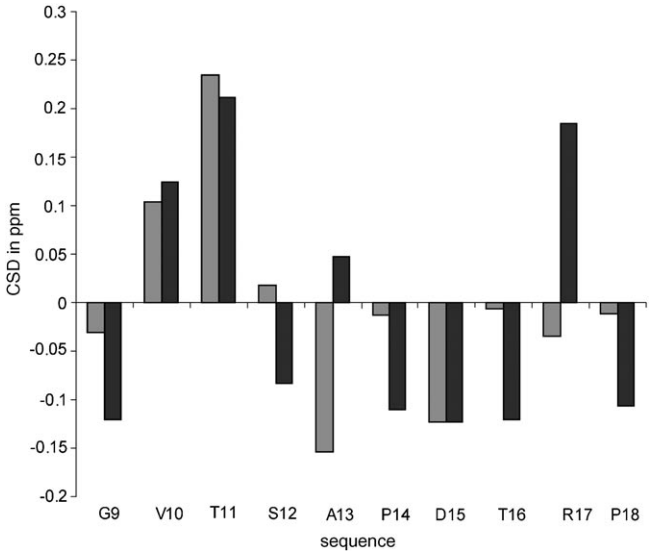

Figure 1. Chemical shift deviations (CSD) of H_α for the glycopeptide **13**. The CSD relative to the values of the unglycosylated peptide **10** is shown in bright grey, while the dark gray color represents the CSD relative to random coil values (helical: −0.39 ppm, extended: +0.37 ppm).

at Thr11 is clearly seen when the differences between the chemical shifts of **13** and **10** are displayed (Figure 1). The comparison with random coil values (δ(**13**)−δ(random coil)) shows a deviation at Ala13, Pro14, Thr16 and Arg17 which can be explained by sequence effects for instance induced by the proline residues Pro14 and Pro18.

Temperature coefficients: The temperature dependence of the NH proton chemical shifts in partially folded peptides is a function of at least two variables: the temperature dependent equilibrium between the folded and random coil states, and the degree of structuring of the folded state at the lower temperature.[40] For unfolded regions, temperature coefficients ($\Delta\delta/\Delta T$) are expected to be between 6 and 10 ppb per K, indicating that the backbone is freely solvated by water and that no hydrogen bonds are present which would protect the backbone amides from proton exchange. In glycopeptide **13** the values of the temperature coefficients were below 5 ppb K^{-1} between residues Val10 and Arg17, suggesting at least partial shielding from solvent and/or hydrogen bonding (Figure 2). The negative $\Delta\delta/\Delta T$ value observed for Thr11 correlated with a downfield shift of the HN resonance of Thr11 in the glycosylated peptide when compared with the non-glycosylated peptide which could be interpreted as a hydrogen bond effect.

Coupling constants: β Turns are characterized by a dihedral angle of $\phi_{i+1} = -60°$, which is consistent with a coupling constant of $^3J_{N\alpha}$ between 4 and 5 Hz, assuming a β turn that is 100% populated. Inverse γ turns show a ϕ_{i+2} of approximately −80° with a coupling constant between 6 and 8 Hz. Because unstructured regions also display values within this range, inverse γ turns cannot be distinguished from random coil on the basis of this coupling constant alone.[41] The high

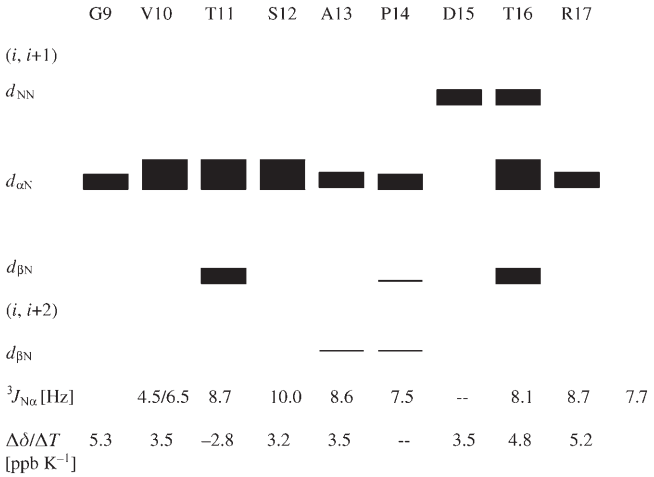

Figure 2. ROE connectivities, $^3J_{N\alpha}$ and temperature coefficients for glycopeptide **13**. The line thickness corresponds to the ROE intensity. In the case of proline, NH refers to δ protons.

value of 10.0 Hz observed for Thr11 in **13** defined a restrained dihedral at the site of glycosylation (Figure 2). The sequence from Val10 to Arg17 exhibited values above 7.5 Hz which indicates either the presence of possibly interconverting turn structures and/or the presence of extended conformations.[38] Considering together the CSD, *J* coupling and temperature coefficients, it appears that the four residues in **13** around the site of glycosylation (Val10, Thr11, Ser12, Ala13) and the neighboured sequence PDTR have a high propensity for an extended and turn structure.

ROE cross peaks: The ROE connectivities were found to be very similar for both peptides except for the glycosylated region in **13**, in which significant differences were observed. In this area, a large number of strong consecutive $d_{\alpha N}(i,i+1)$ connectivities indicated the predominance of extended backbone conformations.[42] The important observation of ROE signals between GalNAc and Gal that clearly indicate the rigidity of the carbohydrate substituent in **13**, prompted us to further investigate this glycopeptide in detail. For this structure, exclusively interresidual ROE contacts are depicted in Figure 3. A significant number of peptide–saccharide ROE signals near the glycosylation site was detected. They include ROE signals between the backbone NH proton of Thr11 and the methyl as well as NH protons of the N-acetyl group of GalNAc, and ROE signals between the β proton and γ proton of Thr11 and the anomeric H1 proton of GalNAc. These ROE interactions suggested that rotation about the α-glycosidic linkage is hindered.

Similar peptide–sugar connectivities have been observed in other NMR studies of α-GalNAc O-glycosylated peptides.[27,32,43] All ROE values used for structure calculation are listed in Table S1 of the Supporting Information.

Conformational analysis of the (2,6)-sialyl-T glycoeicosapeptide 13 by restrained MD calculations: A total of 107 ROE signals were collected for the (2,6)-sialyl-T glycoeicosapeptide **13** and classified into four groups according to their integrated intensities. These distance information in combination with peptide bonds restrained in the *trans* conformation were used as input for a restrained MD simulation. After energy minimization, a final set of eight low energy structures (< 15 kcal mol^{-1}, < 0.05 nm distance restraint violation) was selected.

Two overlapping peptide fragments, GVTSA and APDTR comprising the glycosylated Thr11 with flanking residues, and the immunodominant region PDTR of MUC1, were selected for cluster analysis to determine structural effects of glycosylation. For the GVTSA segment the mean pairwise RMSD for the heavy atoms of these conformers and the corresponding average structure was equal to 0.78 Å. The structural model of **13** exhibits a clearly defined extended, rod-like conformation for the sequence GVTSA (Figure 4).

The directly *O*-linked GalNAc is positioned along one side of an extended β strand formed by the sequence GVTSA. Such positioning is consistent with strong contacts between the *N*-acetyl NH proton of the GalNAc moiety and the amide proton of the glycosylated Thr11 residue and between the methyl group of GalNAc and the H_α and H_β protons of Ala13. Coltart et al.[30] found a similar methyl group association in their study of the glycosylated N-terminal fragment STTAV of the cell surface glycoprotein CD43.

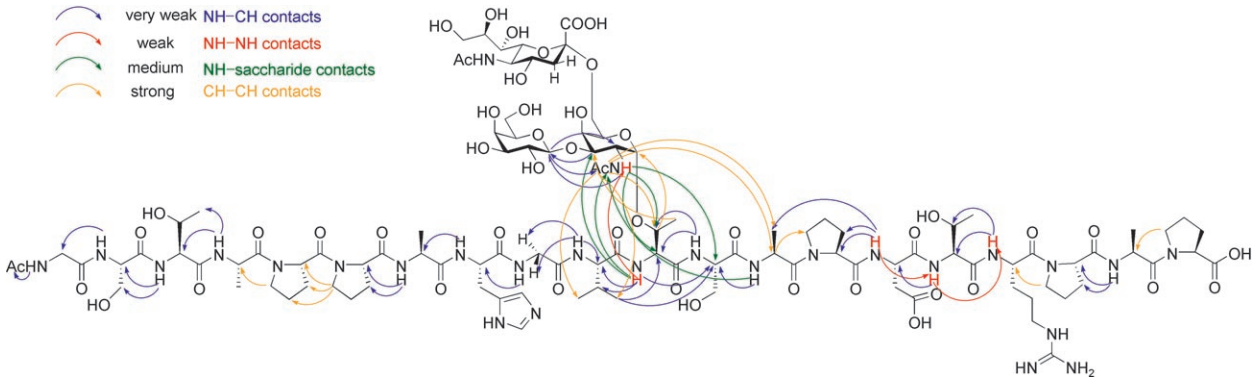

Figure 3. ROE contacts of the glycopeptide **13**.

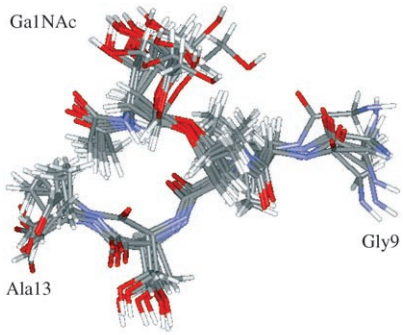

Figure 4. GVTSA sequence of glycopeptide **13** exhibits a rod-like secondary structure. Of the trisaccharide, only GalNAc is shown.

It was suggested by Kirnarsky et al.[32] that the N-acetyl group of the GalNAc moiety interacts directly with the peptide backbone, possibly through hydrogen bonding. An intramolecular hydrogen bonding between the amide proton of GalNAc and the carbonyl oxygen of the O-linked threonine residue was also proposed by Naganagowda et al.[44] as the key stabilizing element, opposed to the O-linked serine analogue for which this interaction seemed to be missing. Our model based on ROE cross peaks clearly indicates a hydrogen bond between the amide proton of GalNAc and the carbonyl oxygen of Thr11 (N–O distance below 2.5 Å, NHO angle $>$ 120°) [ROEs between the NH proton of GalNAc und H_α of Ser12 (medium intensity), H_α of Thr11 (weak intensity) and H_β of Thr11 (weak intensity)].

The structuring effect of the carbohydrates could be explained by the observation that β-branched amino acids favor extended conformations, due to both steric clashes with neighboring side chains and steric clashes with main-chain atoms.[45] Similarly, the attached carbohydrates on Thr11 could act as extremely bulky side chains and influence conformational equilibria of side chain as well as main-chain dihedrals. Schuman et al.[46] concluded in their study of serine trimers substituted by sialyl α(2,6) GalNAc that clustering of more complex carbohydrates shift the conformational equilibrium of the underlying peptide backbone toward a more extended and rigid state.

The analysis of solely monoglycosylated peptides might explain the differing results from Kirnarsky et al.[47] In a recent study on a 21-mer glycosylated with GalNAc, they identified several structural clusters for the GVTSAP sequence by NMR-based molecular modeling comprising turn-like and extended conformations. In a previous report they demonstrated a mostly extended structural shape, termed "γ-turn-like" to indicate that this turn does not fold the peptide chain back.

The significance of our rod-like model of a complex glycopeptide lies in the observation that the inclusion of the tumor-associated Tn carbohydrates at Thr3 and Ser4 upstream from the PDTRP core peptide epitope increased B27.29 antibody binding affinity through direct carbohydrate–antibody interactions.[48] Additionally, Takeuchi et al.[49] showed that the affinity of a sialylated glycopeptide to the anti-MUC1 antibody MY.1E12 was higher than for the analogous glycopeptide without sialylic acid substitution. The latter two findings clearly advocate using complex sugars as epitope-relevant structures.

For the second immunogenically important domain, PDTR, several structural models have been proposed: a type I β turn formed by the residues PDTR[8] and a type II β turn formed by residues APDT were proposed as key element of a knob-like structure.[38,50] The data presented by Kinarsky et al.[32] did not provide direct NMR evidences supporting the existence of either type I or type II β turn. These authors proposed that the PDTR sequence adopts two overlapping inverse γ turns, the first spanning Pro-Asp-Thr and the second Asp-Thr-Arg suggesting a S-shaped bend for the PDTR fragment rather than a knob-like motif.

The strong $d_{NN}(i,i+1)$ connectivities observed by Schuman et al.[28] in their study of 9-residue peptides argued against the existence of two overlapping inverse γ turns, as this arrangement would give rise to only weak $d_{NN}(i,i+1)$ cross peaks between Asp and Thr and between Thr and Arg, corresponding to distances of 3.8 Å in each γ turn. In contrast, the observed NOEs were diagnostic of a type I β turn spanning Pro-Asp-Thr-Arg within the PDTRP peptide epitope region.

With our experimental data obtained under typical bioassay conditions we calculated turn-like structures for the PDTR sequence of **13** (Figure 5). The RMSD of 2.2 Å supports the view of a well-ordered secondary structure in close vicinity to the extended, rod-like conformation of GVTSA.

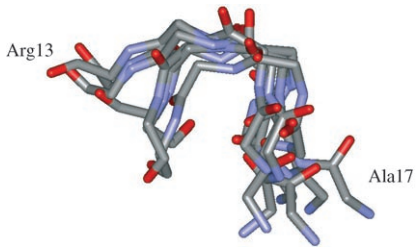

Figure 5. APDTR sequence of glycopeptide **13** exhibits a turn-like structure.

A clear indication of a β-turn structure according to the 7 Å criterion[41] is the $ProC_\alpha$–$ArgC_\alpha$ distance of 5.3 Å in a representative structure of **13**. Although the dihedrals for the $i+1$ and $i+2$ residues of an ideal β turn are not fulfilled [$Asp(\phi_{i+1}) = +66°$, $Asp(\psi_{i+1}) = -84$, $Thr(\phi_{i+1}) = -123°$, $Thr(\psi_{i+1}) = +107$], which correlates to the equatorial position of both side chains in contrast to an axial position for residue $i+2$ in an ideal β turn, the short distance between the C_α of Pro14 and Arg17 and the back folding of the backbone justify the classification as a β turn. A clear distinction between type I and type II can be made by the $H_\alpha(i+1)$–$NH(i+2)$ distance (3.5 and 2.1 Å type II). In the representative structure this distance amounts to 3.6 Å indicating a type I β turn for the sequence PDTR.

A number of different ROE values have been reported. Schuman et al.[28] observed strong NH(i+1)–NH(i+2), NH(i+2)–NH(i+3) and H_β(i+1)–NH(i+2) ROE signals for a 9-residue peptide In the case of **13** the NH ROEs were not strong and the last ROE was missing. Moreover, additional H_β(i+1)–NH(i+3) ROE values were measured for Ala13–Asp15 and Pro14–Thr16 which were also not observed by Kirnarsky et al.[47] studying a 21-mer glycopeptide. The H_α-(i+1)–NH(i+3) cross peak observed by Schuman et al.[28] was not seen in **13**. These differences could be attributed to different test molecules and measurement conditions. Since the glycosylated peptide **13** representing the full length MUC1 repeat sequence was substituted by a complex carbohydrate typically found in cancer-associated cells and was studied under physiological conditions, we are confident to reproduce the conditions relevant for tumour immunotherapy assays. Consequently, our proposed model of a MUC1-derived glycopeptide may give a sound basis for modeling approaches in antibody design.

Experimental Section

General methods: Solvents for moisture-sensitive reactions (acetonitrile, methanol, and dichloromethane) were distilled and dried prior to use according to standard procedures.[51] DMF (amine free, for peptide synthesis) was purchased from Roth, acetic anhydride and pyridine in p.a. quality from Acros. Reagents were purchased at highest available commercial quality and used without further purification unless outlined otherwise. Fmoc-protected amino acids were purchased from Novabiochem. Rapp TentaGel was used as a resin for the solid-phase synthesis. Reactions were monitored by thin-layer chromatography with pre-coated silica gel 60 F_{254} aluminium plates (Merck KGaA, Darmstadt). Flash column chromatography was performed with silica gel (40–63 μm) purchased form Merck KGaA, Darmstadt. Optical rotations $[\alpha]_D$ were measured with a Perkin–Elmer polarimeter 241. RP-HPLC analyses were carried out on a Knauer HPLC system with Phenomenex Luna C18(2) (250×4.6 mm, 5 μ) and Phenomenex Jupiter C18 columns (250×4.6 mm, 5 μ) at a pump rate of 1 mL min^{-1}. Preparative HPLC separations were performed on a Knauer HPLC system with a Phenomenex Luna C18(2) column (250×50 mm, 10 μm) and a pump rate of 20 mL min^{-1}. Semipreparative HPLC separations were carried out on a Knauer HPLC system with Phenomenex Luna C18(2) (250×21.20 mm, 10 μ) and Phenomenex Jupiter (250×21.20 mm, 5 μ) columns at a flow rate of 10 mL min^{-1}. Water and CH_3CN were used as solvents. ^{1}H, ^{13}C, and 2D NMR spectra were recorded on Bruker AC-300, AM-400, ARX-400 or DRX-600 spectrometers. Proton chemical shifts are reported in ppm relative to residual $CHCl_3$ (δ=7.24), DMSO (δ=2.49) or water (δ=4.76). Multiplicities are given as s (singlet), d (doublet), t (triplet), q (quartet), m (multiplet). ^{13}C chemical shifts are reported relative to $CDCl_3$ (δ=77.0) or DMSO (δ=39.5). Assignment of proton and carbon signals was achieved by COSY, TOCSY, HMQC and HMBC experiments when noted. For ^{1}H and ^{13}C signals of the saccharide portions the following denominations were used: *N*-acetyl-D-galactosamine (no apostrophe); D-galactose (′); *N*-acetyl-neuraminic acid (″). MALDI-TOF mass spectra were acquired on a Micromass Tofspec E spectrometer while ESI-mass spectra were obtained on a ThemoQuest-Navigator spectrometer. HR-ESI mass spectra were recorded on a Micromass Q-TOF Ultima spectrometer (matrix: DHB: dihydrobenzoic acid).

***N*-(9*H*-Fluoren-9-yl)methoxycarbonyl-*O*-(2-acetamido-2-deoxy-3-*O*-[2,3,4-tri-*O*-acetyl-6-*O*-benzyl-β-D-galactopyranosyl]-α-D-galactopyranosyl)-L-threonine-*tert*-butylester (5)**: A solution of Fmoc-Thr(βAc_3-6-Bn-Gal(1→3)-α4,6-*O*-Bzn-GalNAc)-O*t*Bu[11] (**4**; 1.00 g, 0.94 mmol) in aqueous acetic acid (80%, 25 mL) was stirred at 80°C for 1 h. Subsequently, the reaction mixture was allowed to cool to 40°C and was diluted by the addition of toluene (25 mL). The solution was concentrated in vacuo and co-evaporated with toluene (5×25 mL). The resulting crude product was purified by flash chromatography (silica gel; cyclohexane/ethyl acetate 1:4; column: h=19 cm, ∅=3 cm) to give the title compound as a colorless, amorphous solid (755 mg, 0.77 mmol, 82%). R_f=0.10 (cyclohexane/ethyl acetate 1:4); $[\alpha]_D^{22}$ = 34.9 (c=1.00, $CHCl_3$); ^{1}H NMR (300 MHz, $CDCl_3$): δ = 7.75 (d, $J_{3,4}=J_{5,6}$=7.4 Hz, 2H, H4-, H5-Fmoc), 7.59 (d, $J_{H1,H2}=J_{H8,H7}$=7.4 Hz, 2H, H1, H8), 7.46–7.15 (m, 9H, H2-, H3-, H6-, H7-Fmoc; 5H, H_{ar}-Bn), 5.95 (d, $J_{NH,H2}$=8.5 Hz, 1H, NH-GalNAc), 5.51 (d, $J_{NH,T\alpha}$=9.2 Hz, 1H, NH-Fmoc), 5.39 (d, $J_{H3',H4'}$=2.9 Hz, 1H, H4′), 5.23–5.08 (m, 1H, H2′), 5.00–4.90 (m, 1H, H3′), 4.80 (br s, 1H, H1), 4.64–4.33 (m, 6H, H1′, H2, CH_2-Fmoc, CH_2-Bn), 4.29–3.98 (m, 5H, H9-Fmoc, T^α, T^β, H4), 3.94–3.56 (m, 5H, $H6_b$, $H6_a$, H5′, H3, H5), 3.55–3.35 (m, 2H, $H6'_a$, $H6'_b$), 2.05, 2.04, 1.98, 1.95 (4×s, 12H, CH_3-Ac), 1.43 (s, 9H, CH_3-*t*Bu), 1.24 (br s, 3H, T^γ); ^{13}C NMR (75.5 MHz, $CDCl_3$, BB): δ = 170.19, 170.10, 169.54 (C=O), 156.37 (C=O urethane), 143.65 (C1a-, C8a-Fmoc), 141.32 (C4a-, C5a-Fmoc), 137.31 (C_q-Bn), 128.51, 128.0 (C_{ar}-Bn), 127.78 (C3-, C6-Fmoc), 127.10 (C2-, C7-Fmoc), 125.18, 124.91 (C1-, C8-Fmoc), 120.07 (C4-, C5-Fmoc), 101.57 (C1′), 100.03 (C1), 83.15 (C_q-*t*Bu), 76.23 (T^β), 76.01 (C3), 73.58 (CH_2-Bn), 72.34 (C5′), 70.85 (C3′), 69.82, 69.54 (C4, C6), 68.72 (C2′), 67.84 (C6′), 67.44 (C4′), 66.83 (CH_2-Fmoc), 62.86 (C5), 59.02 (T^α), 47.59 (C2), 47.24 (C9-Fmoc), 27.95 (CH_3-*t*Bu), 23.23 (CH_3-NHAc), 20.71, 20.61, 20.55 (3×CH_3-OAc), 18.74 (T^γ); HR-ESI-TOF-MS (positive ion mode): m/z: calcd for $C_{50}H_{62}N_2O_{18}Na$: 979.4076; found: 979.4094 $[M+Na]^+$.

***N*-(9*H*-Fluoren-9-yl)methoxycarbonyl-*O*-(2-acetamido-2-deoxy-3-*O*-[2,3,4-tri-*O*-acetyl-6-*O*-benzyl-β-D-galactopyranosyl]-6-*O*-[benzyl-(5-acetamido-4,7,8,9-tetra-*O*-acetyl-3,5-dideoxy-α-D-glycero-D-galacto-2-nonulopyranosyl)onat]-α-D-galactopyranosyl)-L-threonine-*tert*-butylester (7)**: Fmoc-Thr(βAc_3-6-Bn-Gal(1→3)-αGalNAc)-O*t*Bu (**5**; 0.70 g, 0.66 mmol) and αAc_4NeuNAcCOOBnXan[17] (**6**; 1.10 g, 1.64 mmol, 2.5 equiv) were dissolved in a mixture of dry acetonitrile and dry dichloromethane (60 mL, 2:1). The solution was stirred for 1 h in a Schlenk flask (brown glass) in the presence of flame-dried molecular sieves (3 g, powdered, 3 Å) under an argon atmosphere and the exclusion of moisture. After cooling to −65°C, dry silver triflate (421 mg, 1.64 mmol) and a pre-cooled (−10°C) solution of methyl sulfenyl bromide in dry 1,2-dichloroethane[18] (1.03 mL of a 1.6 M solution, 1.64 mmol) were added slowly over 25 min. The reaction mixture was stirred at −68°C for 4 h, subsequently neutralized with Huenig's base (0.33 mL) and allowed to warm to room temperature. The suspension was diluted with dichloromethane (40 mL), filtered through Hyflo Super Cel and concentrated in vacuo. Purification of the crude product by flash chromatography (silica gel; ethyl acetate, column: h=20 cm, ∅=3 cm) gave an anomeric mixture which was separated by preparative RP-HPLC (Phenomenex LUNA, acetonitrile/water 55:45 → 80:20, 60 min; 100:0, 30 min; λ=254 nm, t_R (α anomer)=63.4 min, t_R (β-anomer)=79.0 min) to yield the desired α anomer as a colorless amorphous solid (606 mg, 0.40 mmol, 61%, conversion: 63%). In addition, the β anomer (20 mg, 0.08 mmol, 12%) as the minor component as well as fractions of unreacted **5** (26 mg, 0.027 mmol, 4%) were isolated. α Anomer: R_f=0.21 (ethyl acetate); $[\alpha]_D^{23}$ = 12.2 (c=1.00, $CHCl_3$); t_R=31.8 min (Phenomenex LUNA, acetonitrile/water 55:45 → 75:25, 40 min; 100:0, 20 min, λ=254 nm); ^{1}H NMR (600 MHz, $CDCl_3$, COSY, HMQC, HMBC): δ = 7.79–7.72 (m, 2H, H4-, H5-Fmoc), 7.60 (d, $J_{H1,H2}=J_{H8,H7}$=7.8 Hz, 2H, H1-, H8-Fmoc), 7.44–7.17 (m, 14H, H3-, H6-, H2-, H7-Fmoc; 10H, H_{ar}-Bn), 5.87 (d, $J_{NH,H2}$=8.6 Hz, 1H, NH-GalNAc), 5.50–5.39 (m, 2H, T^{NH} {5.45}, H4′ {5.42}), 5.38–5.24 (m, 2H, H8″ {5.32}, H7″ {5.28}), 5.23–5.06 (m, 4H, CH_2-COO*Bn* {5.18, 5.15}, H2′ {5.13}, NH-NeuNAc {5.09}), 4.95 (dd, $J_{H3',H2'}$=10.3, $J_{H3',H4'}$=3.0 Hz, 1H, H3′), 4.86–4.77 (m, 1H, H4″), 4.71 (d, $J_{H1,H2}$=3.0 Hz, 1H, H1), 4.66–4.44 (m, 5H, H1′ {4.59, d, $J_{H1',H2'}$=8.1 Hz}, H2 {4.49}, CH_2-Fmoc {4.51, 4.47}, CH_{2a}-Bn {4.47}), 4.43–4.31 (m, 1H, CH_{2b}-Bn), 4.30–4.19 (m, 2H, $H9_a''$ {4.27, dd, $J_{H9a'',H9b''}$=12.3, $J_{H9a'',H8''}$=2.3 Hz}, H9-Fmoc {4.24}), 4.18–4.00 (m, 5H, T^α {4.14}, T^β {4.11}, $H9_b''$ {4.05}, H5″ {4.04}, H6″ {4.03}), 3.94–3.73 (m, 4H, H4 {3.90}, $H6_a$ {3.89}, H5′ {3.84}, H5 {3.79}), 3.66–3.57 (m, 1H, H3 {3.61}), 3.55–3.46 (m, 2H, $H6_b$ {3.52}, $H6_a'$ {3.48}), 3.45–3.38 (m, 1H, $H6_b'$ {3.42}), 2.58 (dd, 1H, $J_{H3eq'',H3ax''}$=12.6, $J_{H3eq'',H4''}$=4.3 Hz, $H3_{eq}''$), 2.09, 2.08, 2.05, 2.03, 1.99, 1.98, 1.95 (7×s, 24H, 8×CH_3-Ac), 1.90 (m, 1H, $H3_{ax}''$), 1.84 (s,

3H, CH_3-Ac), 1.42 (s, 9H, CH_3-*t*Bu), 1.26 (d, $J_{T^{\gamma},T^{\beta}}=6.1$ Hz, 3H, T^{γ}); ^{13}C NMR ($CDCl_3$, chemical shifts obtained from HMQC, HMBC): δ = 170.2, 169.5, 169.4, 169.2, 166.7 (C=O), 166.4 (C1″), 155.6 (C=O urethane), 143.0 (C1a-, C8a-Fmoc), 140.5 (C4a-, C5a-Fmoc), 136.7 (C_q-Bn (C6′)), 134.1 (C_q-Bn (C1″)), 127.8, 127.4 (C_{ar}-Bn), 127.2 (C2-, C7-Fmoc), 127.1 (C_{ar}-Bn), 126.3 (C3-, C6-Fmoc), 124.1 (C1-, C8-Fmoc), 119.2 (C4-, C5-Fmoc), 100.8 (C1′), 99.5 (C1), 98.1 (C2″), 82.4 (C_q-*t*Bu), 76.7 (C3), 75.8 (T^{β}), 72.7 (CH_2-Bn (C6′)), 71.9 (C6″), 71.4 (C5′), 70.0 (C3′), 68.4 (C8″), 68.2 (C5), 68.1 (C4″), 68.0 (C2′), 67.5 (C4), 66.9 (CH_2-Bn (C1″)), 66.6 (C4′), 66.6 (C7″), 66.5 (C6′), 66.3 (CH_2-Fmoc), 63.1 (C6), 61.6 (C9″), 58.1 (T^{α}), 48.6 (C5″), 46.9 (C2), 46.6 (C9-Fmoc), 36.8 (C3″), 27.4 (CH_3-*t*Bu), 22.5, 22.3 (CH_3-NHAc), 20.2, 20.0, 19.9, 19.8 (CH_3-OAc), 17.9 (T^{γ}); HR-ES-TOF-MS (positive ion mode): *m*/*z*: calcd for $C_{76}H_{93}N_3O_{30}Na$: 1550.5742, found: 1550.5731 $[M+Na]^+$.

***N*-(9*H*-Fluoren-9-yl)methoxycarbonyl-*O*-(2-acetamido-2-deoxy-3-*O*-[2,3,4-tri-*O*-acetyl-6-*O*-benzyl-β-D-galactopyranosyl]-6-O-[benzyl-(5-acetamido-4,7,8,9-tetra-*O*-acetyl-3,5-dideoxy-α-D-glycero-D-galacto-2-nonulopyranosyl)onat]-α-D-galactopyranosyl)-L-threonine (8)**: A solution of protected trisaccharide **7** (580 mg, 0.394 mmol) in a mixture of TFA (5 mL), dichloromethane (5 mL) and anisole (0.5 mL) was stirred at ambient temperature for 2 h. The reaction mixture was then diluted with toluene (25 mL) and the solvent was removed in vacuo. The resulting residue was co-evaporated with toluene (3×25 mL) and purified by flash chromatography (silica gel; ethyl acetate/ethanol 4:1; column: $h=20$ cm, $\varnothing=3$ cm) and subsequently by preparative RP-HPLC (Phenomenex LUNA, acetonitrile/water 60:40 → 70:30, 70 min; $\lambda=254$ nm, $t_R=46.5$ min) to yield compound **8** (492 mg, 0.334 mmol, 85%) as a colorless, amorphous solid. $R_f=0.51$ (EE/EtOH 2:1); $t_R=17.1$ min (Phenomenex LUNA, acetonitrile/water + 0.1% TFA, 55:45 → 75:25, 30 min; $\lambda=254$ nm); $[\alpha]_D^{22}$ = 24.7 ($c=1.00$, $CHCl_3$); ^1H NMR (400 MHz, $CDCl_3$, COSY, HMQC): δ = 7.78–7.70 (m, 2H, H4-, H5-Fmoc), 7.63–7.52 (m, 2H, H1-, H8-Fmoc), 7.42–7.13 (m, 14H, H3-, H6-, H2-, H7-Fmoc, H_{ar}-Bn (10H)), 6.22 (d, $J_{NH,H2}=8.2$ Hz, 1H, NH-GalNAc), 5.73 (d, $J_{NH,T\alpha}=7.4$ Hz, 1H, NH-Fmoc), 5.44–5.23 (m, 3H, H4′ {5.40}, H8″ {5.33}, H7″ {5.26}), 5.23–5.05 (m, 3H, CH_2-COO*Bn* {5.17, 5.10}, H2′ {5.11}), 5.01–4.72 (m, 3H, H3′ {4.94}, H1 {4.81}, H4″ {4.80}), 4.71 (d, 1H, H1, $J_{H1,H2}=3.0$ Hz), 4.62–4.52 (m, 1H, H1′), 4.51–4.42 (m, 3H, CH_2-Fmoc {4.46}, CH_{2a}-Bn {4.47}), 4.39–4.25 (m, 5H, CH_{2b}-Bn {4.36}, H2 {4.35}, $H9_a''$ {4.30}, T^{α} {4.31}, T^{β} {4.28}), 4.24–4.17 (m, 1H, H9-Fmoc), 4.10–3.72 (m, 7H, $H9_b''$ {4.04}, H6″ {4.04}, H5″ {4.02}, H4 {3.89}, $H6_a$ {3.88}, H5′ {3.82}, H5 {3.79}), 3.71–3.60 (m, 1H, H3), 3.56–3.46 (m, 2H, $H6_b$ {3.50}, $H6_a'$ {3.48}), 3.45–3.32 (m, 1H, $H6_b'$), 2.57 (dd, $J_{H3eq'',H3ax''}=8.8$, $J_{H3eq'',H4''}=3.9$ Hz, 1H, $H3_{eq}''$), 2.15, 2.05, 2.04, 2.02, 1.98, 1.96, 1.94, 1.93 (8×s, 24H, 8×CH_3-Ac), 1.88 (m, 1H, $H3_{ax}''$), 1.85 (s, 3H, CH_3-Ac), 1.21 (d, $J_{T^{\gamma},T^{\beta}}=6.3$ Hz, 3H, T^{γ}); ^{13}C NMR (100.6 MHz, $CDCl_3$, BB, HMQC): δ = 172.70 (COOH), 170.80, 170.27, 170.15, 169.87, 169.64 (C=O), 167.30 (C1″), 155.82 (C=O urethane), 143.78 (C1a-, C8a-Fmoc), 141.25 (C4a-, C5a-Fmoc), 137.25 (C_q-Bn an C6′), 134.83 (C_q-Bn an C1″), 128.73, 128.67, 128.50, 128.43, 128.32, 127.78, 127.67 (C_{ar}-Bn), 127.12 (C2-, C7-Fmoc), 125.03 (C3-, C6-Fmoc), 124.92 (C1-, C8-Fmoc), 119.99 (C4-,C5-Fmoc), 102.11 (C1′), 101.30 (C1), 98.68 (C2″), 78.74 (T^{β}), 77.14 (C3), 73.48 (CH_2-Bn (C6′)), 73.30 (C6″), 72.81 (C5′), 70.82 (C3′), 69.25 (C8″), 68.92 (C5), 68.49 (C4″), 68.17 (C2′), 67.79 (C4), 67.73 (C7″), 67.45 (C6′), 67.02 (CH_2-Fmoc), 67.35 (C4′), 66.70 (CH_2-Bn (C1″)), 63.99 (C6), 62.42 (C9″), 58.66 (T^{α}), 49.25 (C5″), 48.40 (C2), 47.20 (C9-Fmoc), 37.46 (C3″), 23.01, 22.77 (3×CH_3-NHAc), 21.02, 20.70, 20.58, 20.53, 20.47 (7×CH_3-OAc), 18.31 (T^{γ}); HR-ESI-TOF (positive ion mode): *m*/*z*: calcd for $C_{72}H_{85}N_3O_{30}Na$: 1494.5116, found: 1494.5117 $[M+Na]^+$.

General procedure for the automated solid-phase glycopeptide synthesis: Peptide syntheses were performed according to the Fmoc protocol in an automated Perkin–Elmer ABI 433 A peptide synthesizer using Fmoc-Pro-PHB preloaded Tentagel resins.[21] In iterative cycles the peptide sequences were assembled by sequential coupling of the corresponding amino acids. In every coupling step, the *N*-terminal Fmoc group was removed by treatment of the resin (3×2.5 min) with 20% piperidine in *N*-methylpyrrolidone. Amino acid couplings were carried out using Fmoc-protected amino acids (1 mmol) activated by HBTU/HOBt[22] (1 mmol each) and DIPEA (2 mmol) in DMF (20–30 min vortex). After every coupling step, unreacted amino groups were capped by treatment with a mixture of Ac_2O (0.5 M), DIPEA (0.125 M) and HOBt (0.015 M) in NMP (10 min vortex). Attachment of the glycosylated amino acids was performed manually as described in the procedures for the corresponding glycopeptides.

Ac-Gly-Ser-Thr-Ala-Pro-Pro-Ala-His-Gly-Val-Thr-Ser-Ala-Pro-Asp-Thr-Arg-Pro-Ala-Pro-OH (10): Starting from Fmoc-Pro-*O*-Trt preloaded Tentagel S resin[21] **9** (520 mg, 0.094 mmol, loading: 0.18 mmol g^{-1}), the assembly of the eicosapeptide was performed according to the automated standard protocol. After coupling of the final amino acid, Fmoc-Gly-OH, the Fmoc group was cleaved with piperidine (20%) in NMP, and the N-terminus was acetylated with capping reagent on the resin. For the cleavage procedure under simultaneous removal of the acid-labile side-chain protecting groups, the resin was placed into a Merrifield glass reactor, washed with dichloromethane (3×15 mL) and treated with a mixture of trifluoroacetic acid (15.0 mL), distilled water (0.9 mL) and triisopropylsilane (0.9 mL) for 2 h. After filtration, the resin was washed with trifluoroacetic acid (3×3 mL), and the combined filtrates were concentrated in vacuo and co-evaporated with toluene (3×15 mL). The peptide was precipitated by addition of cold (0 °C) diethyl ether (15 mL) to furnish a colorless solid, which was washed with diethyl ether (3×10 mL), dissolved in distilled water and lyophilized. The crude product was purified by preparative RP-HPLC (Phenomenex LUNA C18, acetonitrile/water + 0.1% TFA 5:95 → 45:55; 60 min; $\lambda=212$ nm, $t_R=40.1$ min) to give the title compound (120 mg, 0.062 mmol, 66%) as a colorless solid after lyophilization. $[\alpha]_D^{22}$ = −148.8 ($c=1.00$, H_2O); t_R = 14.3 min (Phenomenex Jupiter C18, CH_3CN/H_2O + 0.1% TFA 5:95 → 45:55, 30 min; λ = 212 nm); ^1H NMR (600 MHz, H_2O/D_2O 9:1, NaH_2PO_4/Na_2HPO_4 buffer, 50 μM, pH 6.50, COSY, TOCSY, ^{15}N HSQC, ^{13}C-HSQC, HMBC, ROESY): δ = 8.55–8.47 (m, 2H, $H(8)^{Im\text{-}H2}$ {s, 8.52}, $D(15)^{NH}$ {8.50}), 8.44–8.09 (m, 12H, $H(8)^{NH}$ {8.38, d, $J_{NH,H\alpha}=7.6$ Hz}, $G(9)^{NH}$ {8.35}, $A(19)^{NH}$ {8.33}, $A(7)^{NH}$ {8.32}, $S(2)^{NH}$ {8.28}, $A(13)^{NH}$ {8.27}, $T(11)^{NH}$ {8.24}, $S(12)^{NH}$ {8.22}, $G(1)^{NH}$ {8.21}, $R(17)^{NH}$ {8.17, d, $J_{NH,r\alpha}=6.9$ Hz}, $A(4)^{NH}$ {8.15}, $T(3)^{NH}$ {8.14}), 8.06 (d, $J_{NH,V\alpha}=7.6$ Hz, 1H, $V(10)^{NH}$}), 7.97 (d, $J_{NH,T\alpha}=7.6$ Hz, 1H, $T(16)^{NH}$), 7.23 (s, 1H, $H(8)^{Im\text{-}H4}$), 7.14–7.06 (m, 1H, $R(17)^{NH\text{-}Gua}$), 4.66–4.42 (m, 8H (signal intensity reduced by H_2O suppression), $D(15)^{\alpha}$ {4.64}, $H(8)^{\alpha}$ {4.62}, $P(5)^{\alpha}$ {4.61}, $R(17)^{\alpha}$ {4.56}, $A(13)^{\alpha}$ {4.52}, $A(4)^{\alpha}$ {4.51}, $A(19)^{\alpha}$ {4.48}, $S(2)^{\alpha}$ {4.46}), 4.39–4.21 (m, 8H, $S(12)^{\alpha}$ {4.37}, $T(11)^{\alpha}$ {4.33}, $P(18)^{\alpha}$ {4.33}, $P(14)^{\alpha}$ {4.32}, $P(20)^{\alpha}$ {4.31}, $P(6)^{\alpha}$ {4.29}, $T(3)^{\alpha}$ {4.27}, $T(16)^{\alpha}$ {4.24}), 4.20–4.09 (m, 5H, $T(3)^{\beta}$ {4.16}, $A(7)^{\alpha}$ {4.15}, $V(10)^{\alpha}$ {4.14}, $T(11)^{\beta}$ {4.14}, $T(16)^{\beta}$ {4.13}), 3.98–3.65 (m, 13H, $G(9)^{\alpha a}$ {3.92}, $G(1)^{\alpha}$ {3.89}, $S(12)^{\beta a}$ {3.89}, $G(9)^{\alpha b}$ {3.87}, $S(2)^{\beta a}$ {3.82}, $S(2)^{\beta b}$ {3.78}, $S(12)^{\beta b}$ {3.75}, $P(5)^{\delta a}$ {3.74}, $P(6)^{\delta a}$ {3.73}, $P(14)^{\delta a}$ {3.72}, $P(18)^{\delta a}$ {3.73}, $P(20)^{\delta a}$ {3.69}, $P(14)^{\delta b}$ {3.53}), 3.63–3.45 (m, 4H, $P(20)^{\delta b}$ {3.58}, $P(6)^{\delta b}$ {3.58}, $P(5)^{\delta b}$ {3.53}, $P(18)^{\delta b}$ {3.53}), 3.21 (dd, 1H, $H8^{\beta a}$, $J_{H\beta a,H\beta b}=15.6$ Hz, $J_{H\beta,H\alpha}=5.9$ Hz), 3.17–3.04 (m, 3H, $R(17)^{\delta}$ {3.13}, $H(8)^{\beta b}$ {3.11}), 2.87 (dd, $J_{D\beta a,D\beta b}=16.9$, $J_{H\beta,H\alpha}=6.6$ Hz, 1H, $D(15)^{\beta a}$), 2.79 (dd, $J_{D\beta a,D\beta b}=17.1$, $J_{H\beta,H\alpha}=6.9$ Hz, 1H, $D(15)^{\beta b}$), 2.32–2.13 (m, 5H, $P(5)^{\beta a}$ {2.26}, $P(14)^{\beta a}$ {2.19}, $P(18)^{\beta a}$ {2.19}, $P(20)^{\beta a}$ {2.22}, $P(6)^{\beta a}$ {2.18}), 2.07–1.99 (m, 1H, $V(10)^{\beta}$ {2.02}), 1.99–1.70 (m, 19H, $AcNH^{terminal}$ (1.97, s), $P(5)^{\gamma}$ {1.95}, $P(20)^{\gamma}$ {1.95}, $P(14)^{\gamma}$ {1.95}, $P(6)^{\gamma}$ {1.93}, $P(18)^{\gamma}$ {1.93}, $P(20)^{\beta b}$ {1.92}, $P(14)^{\beta b}$ {1.83}, $P(5)^{\beta b}$ {1.79}, $P(18)^{\beta b}$ {1.80}, $P(6)^{\beta b}$ {1.76}, $R(17)^{\beta a}$ {1.76}), 1.70–1.51 (m, 3H, $R(17)^{\beta b}$ {1.66}, $R(17)^{\gamma}$ {1.58}), 1.33–1.19 (m, 12H, $A(19)^{\beta}$ {1.28}, $A(13)^{\beta}$ {1.28}, $A(4)^{\beta}$ {1.25}, $A(7)^{\beta}$ {1.24}), 1.15–1.04 (m, 9H, $T(11)^{\gamma}$ {1.12}, $T(3)^{\gamma}$ {1.11}, $T(16)^{\gamma}$ {1.10}), 0.85 (t, 6H, $V(10)^{\gamma}$, $J_{V\gamma,V\beta}=6.3$ Hz); ^{13}C NMR (chemical shifts taken from ^{13}C-HSQC and HMBC): δ = 176.21 ($P(20)^{C=O}$), 174.89 ($A(7)^{C=O}$), 174.05 ($P(14)^{C=O}$), 174.04 ($P(6)^{C=O}$), 173.78 ($V(10)^{C=O}$), 173.54 ($P(18)^{C=O}$), 172.61 ($D(15)^{COOH}$), 172.18 ($S(2)^{C=O}$), 172.01 ($H(8)^{C=O}$), 171.87 ($P(5)^{C=O}$), 171.64 ($T(11)^{C=O}$), 171.31 ($T(16)^{C=O}$), 171.19 ($T(3)^{C=O}$), 171.22 ($R(17)^{C=O}$), 171.20 ($G(9)^{C=O}$), 133.67 ($H(8)^{Im\text{-}C2}$), 128.39 ($H(8)^{Im\text{-}C5}$), 117.42 ($H(8)^{Im\text{-}C4}$), 67.07 ($T(11)^{\beta}$), 67.07 ($T(3)^{\beta}$), 67.07 ($T(16)^{\beta}$), 61.25 ($S(12)^{\beta}$), 61.12 ($S(2)^{\beta}$), 60.35 ($P(18)^{\alpha}$), 60.32 ($P(14)^{\alpha}$), 60.06 ($P(6)^{\alpha}$), 59.85 ($P(20)^{\alpha}$), 59.57 ($V(10)^{\alpha}$), 58.99 ($T(16)^{\alpha}$), 58.97 ($T(11)^{\alpha}$), 58.83 ($T(3)^{\alpha}$), $(P(5)^{\alpha})^{\S}$, 55.50 ($S(2)^{\alpha}$), 55.32 ($S(12)^{\alpha}$), $(H(8)^{\alpha})^{\S}$, $(D(15)^{\alpha})^{\S}$, 51.08 ($R(17)^{\alpha}$), 47.85 ($A(13)^{\alpha}$), 49.70 ($A(7)^{\alpha}$), 47.82 ($A(4)^{\alpha}$), 47.65 ($A(19)^{\alpha}$), 48.51 ($P(6)^{\delta}$), 47.73# ($P(5)^{\delta}$, $P(18)^{\delta}$), 47.65 ($P(14)^{\delta}$), 47.44 ($P(20)^{\delta}$), 42.45 ($G(1)^{\alpha}$), 40.61 ($R(17)^{\delta}$), 35.19 ($D(15)^{\beta}$), 30.18 ($V(10)^{\beta}$), 29.29 ($P(14)^{\beta}$), 29.28 ($P(6)^{\beta}$), 29.28 ($P(18)^{\beta}$), 28.88 ($P(20)^{\beta}$), 27.98 ($P(5)^{\beta}$), 27.46 ($R(17)^{\beta}$), 26.34 ($H(8)^{\beta}$), 24.55# ($P(5)^{\gamma}$, $P(6)^{\gamma}$, $P(14)^{\gamma}$, $P(18)^{\gamma}$, $P(20)^{\gamma}$), 23.98 ($R(17)^{\gamma}$), 21.61

($AcNH^{terminal}$), 18.83 ($T(16)^{\gamma}$), 18.74 ($T(3)^{\gamma}$), 18.74 ($T(11)^{\gamma}$), 18.39 ($V(10)^{\gamma a}$), 17.61 ($V(10)^{\gamma b}$), 16.40 ($A(7)^{\beta}$), 15.38 ($A(13)^{\beta}$), 15.36 ($A(4)^{\beta}$), 15.16 ($A(19)^{\beta}$); [§]: annihilated by H_2O suppression, [#]: signals overlapped; MALDI-TOF-MS (DHB, positive ion mode): *m/z*: calcd for $C_{82}H_{130}N_{25}O_{29}$: 1930.1, found: 1930.2 $[M+H]^+$, 1952.2 $[M+Na]^+$, 1968.2 $[M+K]^+$, 1974.3 $[M+2Na-H]^+$.

Fmoc-Ser(*t*Bu)-Ala-Pro-Asp(O*t*Bu)-Thr(*t*Bu)-Arg(Pmc)-Pro-Ala-Pro-Trt-Tg (11): The resin-bound peptide fragment was prepared in a 41 mL reaction vessel of peptide synthesizer according to the standard procedure starting from the Fmoc-Pro-O-Trt preloaded Tentagel S resin **9a**[21] (1.38 g, 0.28 mmol, loading: 0.20 mmol g^{-1}) and using the FastMoc (0.25 mmol) protocol for amino acid couplings. After coupling of the last amino acid, Fmoc-Ser(*t*Bu)-OH, the resin was thoroughly washed with NMP and dichloromethane and dried under a nitrogen flow. Residual solvent was removed in high vacuum to give 1.55 g dry resin, which was used in the syntheses of different glycopeptide structures.

Ac-Gly-Ser-Thr-Ala-Pro-Pro-Ala-His-Gly-Val-Thr(βAc$_3$BnGal-(1→3)-[αAc$_4$NeuNAcCOOBn-(2→6)]-αGalNAc)-Ser-Ala-Pro-Asp-Thr-Arg-Pro-Ala-Pro-OH (12): A portion of the functionalized Tentagel resin **11** (282 mg, max. 0.05 mmol) was treated in the peptide synthesizer with piperidine (20%) in NMP to remove the temporary Fmoc-protecting group. Subsequently, a solution of the (2,6)-sialyl-T threonine building block **8** (125 mg, 0.085 mmol, 1.7 equiv), HATU[24] (34 mg, 0.090 mmol, 1.8 equiv), HOAt (12 mg, 0.090 mmol, 1.8 equiv) and *N*-methylmorpholine (19.8 μL, 0.18 mmol, 3.6 equiv) in NMP (2 mL) was added to the resin. After shaking for 4 h, excess reagents were removed by filtration and the resin was washed with NMP. Remaining unreacted amino groups were acetylated with capping reagent. The eicosapeptide sequence was completed resuming the automated standard procedure according to the Fmoc protocol. After coupling of the last amino acid, the terminal Fmoc group was exchanged for an acetyl group and the resin was treated with a mixture of TFA (15 mL), distilled water (0.9 mL) and triisopropylsilane (0.9 mL) for simultaneous cleavage of the linker and the acid-labile side-chain protecting groups. Subsequently, the resin was washed with trifluoroacetic acid (3×3 mL), the combined filtrates were concentrated in vacuo and co-evaporated with toluene (3×15 mL). The peptide was precipitated by addition of cold (0°C) diethyl ether (15 mL) to give a colorless solid, which was washed with diethyl ether (3×10 mL), dissolved in distilled water and lyophilized. The crude material was purified by preparative RP-HPLC (Phenomenex Jupiter C18, grad.: acetonitrile/water + 0.1% TFA 25:75 → 50:50, 80 min, λ=212 nm, t_R=28.1 min) to furnish the partially protected glycopeptide **12** as a colorless lyophilizate (66 mg, 0.022 mmol, 44%). $[\alpha]_D^{23}=-63.8$ (c=1.00, methanol); t_R=26.6 min (Phenomenex Luna C18(2), gradient: acetonitrile/water + 0.1% TFA 15:85 → 45:55, 30 min, λ=212 nm); MALDI-TOF-MS (DHB, positive ion mode): *m/z*: calcd for $C_{135}H_{195}N_{27}O_{54}$: 3060.1, found 3059.9 $[M]^+$, 3082.0 $[M+Na]^+$, 3104.0 $[M+2Na-H]^+$.

Ac-Gly-Ser-Thr-Ala-Pro-Pro-Ala-His-Gly-Val-Thr(βAc$_3$Gal-(1→3)-[αAc$_4$NeuNAc COOH-(2→6)]-αGalNAc)-Ser-Ala-Pro-Asp-Thr-Arg-Pro-Ala-Pro-OH: For the removal of the benzyl groups, the (2,6)-sialyl-T glycopeptide **12** (73 mg, 0.024 mmol) was dissolved in anhydrous methanol (20 mL), and a catalytic amount of 5% palladium on activated charcoal was added under argon. The reaction flask was subsequently purged with H_2 and the suspension was stirred for 21 h under H_2 atmosphere. The charcoal was removed by filtration through Hyflo Super Cell which was washed with methanol (50 mL) afterwards. The combined filtrates were concentrated in vacuo, dissolved in distilled water (5 mL) and lyophilized to give the debenzylated glycopeptide (65 mg, max. 0.223 mmol) as a colorless lyophilizate, which was employed for the final deprotection without further purification. t_R=12.5 min (Phenomenex Jupiter C18, gradient: acetonitrile/water + 0.1% TFA 15:85 → 45:55, 30 min, λ=212 nm); MALDI-TOF-MS (DHB, positive ion mode): *m/z*: calcd for $C_{121}H_{184}N_{27}O_{54}$: 2880.9, found: 2880.8 $[M+H]^+$, 2902.5 $[M+Na]^+$, 2918.5 $[M+K]^+$, 2924.4 $[M+2Na-H]^+$.

Ac-Gly-Ser-Thr-Ala-Pro-Pro-Ala-His-Gly-Val-Thr(βGal-(1→3)-[αNeuNAcCOOH-(2→6)]-αGalNAc)-Ser-Ala-Pro-Asp-Thr-Arg-Pro-Ala-Pro-OH (13): The crude, debenzylated (2,6)-sialyl-T eicosapeptide (65 mg, max. 0.223 mmol) was dissolved in anhydrous methanol (20 mL) and treated with a solution of 1% sodium methoxide in methanol until a pH of 9.5 was reached. The reaction mixture was stirred for 16 h at ambient temperature and was then neutralized by the addition of acetic acid (0.05 mL). The solvent was removed in vacuo, and the resulting residue was purified by preparative RP-HPLC (Phenomenex Jupiter C18, gradient: acetonitrile/water + 0.1% TFA 5:95 → 30:70, 60 min, λ=212 nm, t_R=24.8 min), the deprotected MUC1 glycoeicosapeptide **13** (34 mg, 0.013 mmol, 55% over two steps) was isolated as colorless lyophilizate. $[\alpha]_D^{23}=-107.3$ (c=1.00, H_2O); t_R=14.2 min (Phenomenex Jupiter C18, gradient: acetonitrile/water + 0.1% TFA 5:95 → 30:70, 30 min, λ=212 nm); ^{1}H NMR (600 MHz, [D$_6$]DMSO, COSY, TOCSY, HMQC, HMBC, ROESY, NOESY): δ = 8.93 (s, 1H, $H(8)^{Im\text{-}H2}$), 8.27–8.20 (m, 2H, $D(15)^{NH}$ {8.24}, $G(9)^{NH}$ {8.22}), 8.17–8.06 (m, 10H, $S(12)^{NH}$ {8.12}, $A(19)^{NH}$ {8.11}, $T(11)^{*NH}$ {8.10}, $H(8)^{NH}$ {8.08}, $G(1)^{NH}$ {8.12}, $A(7)^{NH}$ {8.04}, NH-NeuNAc {8.02}, $S(2)^{NH}$ {7.96}, $V(10)^{NH}$ {7.94}, $A(13)^{NH}$ {7.88}), 7.82 (d, 1H, $A(4)^{NH}$, $J_{NH,A\alpha}$=6.9 Hz), 7.71 (d, 1H, $T(16)^{NH}$, $J_{NH,T\alpha}$=8.5 Hz), 7.49 (d, 1H, $R(17)^{NH}$, $J_{NH,R\alpha}$=3.8 Hz), 7.36 (s, 1H, $H(8)^{Im\text{-}H4}$), 7.32 (d, 1H, $T(3)^{NH}$, $J_{NH,T\alpha}$=7.9 Hz), 7.21 (s_b, 1H, OH), 7.13 (d, 1H, OH, J=1.5 Hz), 7.06–6.99 (m, 2H, NH-GalNAc, OH), 4.82 (d, 1H, H1, $J_{H1,H2}$=2.1 Hz), 4.60–4.41 (m, 7H, $H(8)^{\alpha}$ {4.57}, $V(10)^{\alpha}$ {4.52}, $D(15)^{\alpha}$ {4.50}, $A(4)^{\alpha}$ {4.49} $R(17)^{\alpha}$ {4.48}, $A(19)^{\alpha}$ {4.46}, $T(11)^{*\alpha}$ {4.45}), 4.40–4.25 (m, 6H, 3×P^{α} {4.34, 4.29, 4.26}, $A(13)^{\alpha}$ {4.37}, $S(2)^{\alpha}$ {4.37}, $S(12)^{\alpha}$ {4.28}), 4.23–4.07 (m, 8H, 2×P^{δ} {4.22, 4.17}, $T(3)^{\alpha}$ {4.19}, H1′ {4.18}, $T(16)^{\alpha}$ {4.17}, $T(11)^{*\beta}$ {4.16}, H2 {4.10}, $A(7)^{\alpha}$ {4.15}), 4.07–4.01 (m, 2H, $T(16)^{\beta}$ {4.04}, OH), 3.97–3.91 (m, 2H, $T(3)^{\beta}$ {3.95}, H4′ {3.93}), 3.90–3.81 (m, 5H, $G(9)^{\alpha a}$ {3.86}, H5 {3.84}, H4 {3.83}, OH), 3.80–3.27 (m, 31H, $G(9)^{\alpha b}$ {3.76}, $G(1)^{\alpha}$ {3.73}, $H6_a$ {3.73}, H3 {3.67}, 5×P^{δ} {3.64, 3.63, 3.57, 3.50, 3.44}, H7″ {3.61}, H4″ {3.55}, $S(2)^{\beta a}$ {3.61}, $H9_a''$ {3.61}, $S(12)^{\beta}$ {3.53}, $S(2)^{\beta b}$ {3.52}, $H6_a'$ {3.52}, H5″ {3.48}, $H6_b$ {3.44}, $H6_b'$ {2.47}, $H9_b''$ {3.38}, H6″ {3.33}, H2′ {3.30}, H8″ {3.30}, H5′ {3.30}), 3.25–3.20 (m, 1H, H3′), 3.15–3.02 (m, 3H, $H(8)^{\beta\alpha}$ {3.11}, $R(17)^{\delta}$ {3.08}), 3.00–2.92 (m, 1H, $H8^{\beta b}$), 2.72 (dd, 1H, $D(15)^{\beta b}$, $J_{D\beta\alpha,D\beta b}$=16.4 Hz, $J_{D\beta,D\alpha}$=5.9 Hz), 2.54–2.46 (m, 2H (partially covered by DMSO signal), $D(15)^{\beta b}$ {2.51), $H3_{eq}''$ {2.49}), 2.17–2.08 (m, 2H, 2×$P^{\beta a}$ {2.13}, {2.12}), 2.06–1.65 (m, 29H, 2×$P^{\beta a}$ {2.01, 1.98}, $V(10)^{\beta}$ {1.95}, 5×P^{γ} {1.89, 1.88, 1.87, 1.86, 1.84}, P^{β} {1.83}, 4×$P^{\beta b}$ {1.82, 1.77, 1.76, 1.75}, $AcNH''$ {s, 1.87, 3H), $AcNH^{terminal}$ (s, 1.85, 3H), $AcNH^{GalNAc}$ (s, 1.82, 3H), $R^{\beta a}$ {1.68}), 1.56–1.46 (m, 3H, $R(17)^{\beta b}$ {1.51}, $R(17)^{\gamma}$ {1.51}, $H3_{ax}''$ {1.50}), 1.22–1.10 (m, 15H, $A(7)^{\beta}$ {1.19}, $A(19)^{\beta}$ {1.18}, $A(4)^{\beta}$ {1.16}, $T(16)^{\gamma}$ {1.15}, $A(13)^{\beta}$ {1.14}), 1.01 (d, 3H, $T(11)^{*\gamma}$, $J_{T\gamma,T\beta}$=6.1 Hz), 0.99 (d, 3H, $T(3)^{\gamma}$, $J_{T\gamma,T\beta}$=6.1 Hz), 0.90 (d, 3H, $V(10)^{\gamma a}$, $J_{V\gamma,V\beta}$=6.4 Hz), 0.84 (d, 3H, $V(10)^{\gamma b}$, $J_{V\gamma,V\beta}$=6.7 Hz); ^{13}C NMR (chemical shifts obtained from ^{13}C-HSQC and HMBC): δ = 173.35, 172.64, 171.93, 171.86, 171.14, 170.50, 170.43, 170.39, 170.35, 170.00, 169.66, 169.55, 169.35 (C=O), 170.67 (C1″), 133.94 ($H(8)^{C4}$), 117.26 ($H(8)^{C4}$), 105.01 (C1′), 98.95 (C1), 98.29 C(2″), 77.98 (C3), 75.72 ($T(11)^{*\beta}$), 75.55 (C5′), 73.71 (C6″), 73.22 (C3′), 71.52 (C7″), 70.80 (C2′), 68.65 (C8″), 68.34 (C4), 68.32 (C5), 66.95 (C4′), 66.95 ($T(3)^{\beta}$), 66.48 (C4″), 66.45 ($T(16)^{\beta}$), 63.76 (C6), 63.17 (C9″), 61.95 ($S(12)^{\beta}$), 61.90 ($S(2)^{\beta}$), 60.70 (C6′), 59.54, 59.29, 59.25, 58.76, 58.04 (5×P^{α}), 58.75 ($T(11)^{*\alpha}$), 58.60 ($T(3)^{\alpha}$), 58.09 ($T(16)^{\alpha}$), 57.38 ($V(10)^{\alpha}$), 55.10 ($S(12)^{\alpha}$), 55.05 ($S(2)^{\alpha}$), 52.48 (C5″), 51.62 ($H(8)^{\alpha}$), 50.55 ($R(17)^{\alpha}$), 50.15 ($D(15)^{\alpha}$), 48.61 ($A(7)^{\alpha}$), 48.21 (C2), 46.53 ($A(7)^{\alpha}$), 46.42 ($A(4)^{\alpha}$), 46.94, 46.92, 46.80, 46.77, 46.50 (5×$P(5)^{\delta}$), 42.22 ($G(9)^{\alpha}$), 40.78 (C3″), 40.77 ($R(17)^{\delta}$), 35.76 ($D(15)^{\beta}$), 31.33 ($V(10)^{\beta}$), 29.22, 29.16, 28.85, 28.82, 28.00 (5×P^{β}), 28.48 ($R(17)^{\beta}$), 27.13 ($H(8)^{\beta}$), 24.8–24.4 (5×P^{γ})[#], 24.66 ($R(17)^{\gamma}$), 22.85 ($AcNH''$), 22.69 ($AcNH^{GalNAc}$), 22.69 ($AcNH^{terminal}$), 20.00 ($T(11)^{*\gamma}$), 19.85 ($T(3)^{\gamma}$), 19.33 ($V(10)^{\gamma a}$), 18.70 ($A(13)^{\beta}$), 18.60 ($A(4)^{\beta}$), 18.48 ($V(10)^{\gamma b}$), 18.42 ($T(16)^{\gamma}$), 17.81 ($A(7)^{\beta}$), 16.87 ($A(19)^{\beta}$); ^{1}H NMR (600 MHz, H_2O/D_2O 9:1, NaH_2PO_4/Na_2HPO_4 buffer, 50 μM, pH 6.50, COSY, TOCSY, ^{15}N-HSQC, ^{13}C-HSQC, HMBC, ROESY): δ=8.66 (d, 1H, $T^*(11)^{NH}$, $J_{NH,T\alpha}$=7.9 Hz), 8.51–7.87 (m, 16H, $S(12)^{NH}$ {8.45}, $A(13)^{NH}$ {8.43}, $D(15)^{NH}$ {8.38}, $H(8)^{H2}$ {8.38}, G(9) {8.33}, $H(8)^{NH}$ {8.33}, $A(7)^{NH}$ {8.32}, $S(2)^{NH}$ {8.28}, $A(19)^{NH}$ {8.24}, G(1) {8.22}, $R(17)^{NH}$ {8.18}, $A(4)^{NH}$ {8.15}, $T(3)^{NH}$ {8.15}, $V(10)^{NH}$ {8.02, d, $J_{NH,V\alpha}$=6.9 Hz}, $T(16)^{NH}$ {7.95}, NH-NeuNAc {7.95}), 7.54 (d, 1H, NH-GalNAc, $J_{NH,H1}$=9.9 Hz), 7.28–7.13 (m, 2H, $R(17)^{NH\text{-}Gua}$ {7.24}, $H(8)^{H4}$ {7.19}), 4.86 (m, 1H, H1 (partially covered by H_2O signal)), 4.63–4.35 (m, 10H (partially covered by H_2O signal), $P(5)^{\alpha}$ {4.61}, $H(8)^{\alpha}$ {4.59}, $T(11)^{*\alpha}$ {4.56}, $R(17)^{\alpha}$ {4.53}, $D(15)^{\alpha}$ {4.52}, $A(4)^{\alpha}$ {4.51}, $A(19)^{\alpha}$ {4.48}, $S(2)^{\alpha}$ {4.45}, $S(12)^{\alpha}$ {4.39}, $A(13)^{\alpha}$ {4.37}), 4.34–4.20 (m, 8H, H1′ {4.33}, $P(18)^{\alpha}$ {4.31},

P(14)$^{\alpha}$ {4.31}, P(6)$^{\alpha}$ {4.29}, T(3)$^{\alpha}$ {4.27}, V(10)$^{\alpha}$ {4.24}, T(16)$^{\alpha}$ {4.23}, T(11)$^{*\beta}$ {4.22}), 4.19–3.97 (m, 7H, T(3)$^{\beta}$ {4.15}, A(7)$^{\alpha}$ {4.14}, P(20)$^{\alpha}$ {4.14}, T(16)$^{\beta}$ {4.14}, H2 {4.13}, H4 {4.09}, H5 {4.01}), 3.97–3.32 (m, 34H, G(9)$^{\alpha a}$ {3.91}, H3 {3.90}, G(1)$^{\alpha}$ {3.89}, G(9)$^{\alpha b}$ {3.84}, H6$_a$ {3.83}, S(2)$^{\beta a}$ {3.82}, H4′ {3.80} H7″ {3.79}, S(2)$^{\beta b}$ {3.78}, H9$_a$″ {3.77}, S(12)$^{\beta a}$ {3.76}, H5″ {3.73}, P(5)$^{\delta a}$ {3.73}, P(14)$^{\delta a}$ {3.73}, P(18)$^{\delta a}$ {3.73}, P(6)$^{\delta a}$ {3.72}, S(12)$^{\beta b}$ {3.69}, H6$_a$′ {3.68}, P(20)$^{\delta a}$ {3.65}, H6$_b$′ {3.63}, H6″ {3.60}, P(14)$^{\delta b}$ {3.57}, H4″ {3.56}, H9$_b$″ {3.55}, P(20)$^{\delta b}$ {3.54}, P(6)$^{\delta b}$ {3.53}, P(5)$^{\delta b}$ {3.53}, H5′ {3.53}, P(18)$^{\delta b}$ {3.53}, H3′ {3.50}, H8″ {3.48}, H6$_b$ {3.48}, H2′ {3.41}), 3.25–3.02 (m, 4H, H(8)$^{\beta a}$ {3.19}, R(17)$^{\delta}$ {3.13}, H(8)$^{\beta b}$ {3.10}), 2.70–2.51 (m, 3H, D(15)$^{\beta a}$ {2.64}, H3$_{eq}$″ {2.58}, D(15)$^{\beta b}$ {2.57}), 2.31–2.08 (m, 5H, P(5)$^{\beta a}$ {2.26}, P(14)$^{\beta a}$ {2.22}, P(18)$^{\beta a}$ {2.19}, P(6)$^{\beta a}$ {2.18}, P(20)$^{\beta a}$ {2.12}), 1.96 (s, 3H, AcNH^{terminal}), 1.93 (s, 3H, AcNH″), 1.92 (s, 3H, AcNH^{GalNAc}), 2.05–1.45 (m, 23H, V(10)$^{\beta}$ {2.01}, P(14)$^{\gamma}$ {1.96}, P(5)$^{\gamma}$ {1.94}, P(6)$^{\gamma}$ {1.92}, P(18)$^{\gamma}$ {1.91}, P(20)$^{\gamma}$ {1.89}, P(14)$^{\beta b}$ {1.84}, P(5)$^{\beta b}$ {1.80}, P(18)$^{\beta b}$ {1.81}, P(20)$^{\beta b}$ {1.81}, P(6)$^{\beta b}$ {1.75}, R(17)$^{\beta a}$ {1.75}, R(17)$^{\beta b}$ {1.68}, R(17)$^{\gamma}$ {1.59}, H3$_{ax}$″ {1.54}), 1.36–1.15 (m, 15H, A(13)$^{\beta}$ {1.30}, A(19)$^{\beta}$ {1.28}, A(4)$^{\beta}$ {1.25}, A(7)$^{\beta}$ {1.24}, T(11)$^{*\gamma}$ {1.22}), 1.15–1.01 (m, 6H, T(3)$^{\gamma}$ {1.11}, T(16)$^{\gamma}$ {1.10}), 0.89 (d, 3H, V(10)$^{\gamma a}$, $J_{V\gamma,V\beta}$ = 6.9 Hz), 0.87 (d, 3H, V(10)$^{\gamma b}$, $J_{V\gamma,V\beta}$ = 6.6 Hz); ^{13}C NMR (chemical shifts obtained from ^{13}C-HMQC and HMBC): δ = 174.93, 174.90, 173.95, 173.76, 173.66, 173.61, 173.53, 173.34, 171.61, 171.25, 170.94, 170.62 (C=O), 173.24 (C1″), 134.15 (H(8)^{C2}), 117.63 (H(8)^{C4}), 104.70 (C1′), 100.07 C(2″), 99.31 (C1), 77.44 (T(11)$^{*\beta}$), 77.16 (C3), 74.91 (C5′), 72.63 (C3′), 72.49 (C6″), 71.77 (C7″), 70.65 (C2′), 69.63 (C8″), 68.99 (C4), 68.64 (C4′), 68.26 (C5), 68.26 (C4″), 66.95 (T(3)$^{\beta}$), 66.95 (T(16)$^{\beta}$), 63.85 (C9″), 62.65 (C6), 61.89 (P(20)$^{\alpha}$), 61.50 (S(12)$^{\beta}$), 61.05 (C6′), 61.04 (S(2)$^{\beta}$), 60.3 (P(18)$^{\alpha}$), 60.2 (P(14)$^{\alpha}$), 60.05 (P(6)$^{\alpha}$), 59.28 (V(10)$^{\alpha}$), 58.88 (T(16)$^{\alpha}$), 58.87 (T(3)$^{\alpha}$), 58.57 (P(5)$^{\alpha}$), 57.11 (T(11)$^{*\alpha}$), 55.49 (S(2)$^{\alpha}$), 54.96 (S(12)$^{\alpha}$), 52.49 (H(8)$^{\alpha}$), 51.85 (C5″), 51.4 (D(15)$^{\alpha}$), 51.38 (R(17)$^{\alpha}$), 48.26 (C2), 48.20 (A(7)$^{\alpha}$), 47.75 (A(13)$^{\alpha}$), 47.68 (A(4)$^{\alpha}$), 47.8 (P(5)$^{\delta}$, P(14)$^{\delta}$)$^{\#}$, 47.6 (P(6)$^{\delta}$), 47.6 (P(18)$^{\delta}$), 47.46 (A(19)$^{\alpha}$), 47.4 (P(20)$^{\delta}$), 42.52 (G(1)$^{\alpha}$), 40.56 (R(17)$^{\delta}$), 40.15 (C3″), 38.08 (D(15)$^{\beta}$), 30.13 (V(10)$^{\beta}$), 29.22 (P(18)$^{\beta}$), 29.19 (P(20)$^{\beta}$), 29.11 (P(6)$^{\beta}$), 29.11 (R(17)$^{\beta}$), 27.82 (P(5)$^{\beta}$), 26.59 (H(8)$^{\beta}$), 24.50 (P(5)$^{\gamma}$), 24.50 (P(6)$^{\gamma}$), 24.50 (P(14)$^{\gamma}$), 24.50 (P(18)$^{\gamma}$), 24.39 (P(20)$^{\gamma}$), 23.81 (R(17)$^{\gamma}$), 22.03 (AcNH^{GalNAc}), 21.90 (AcNH″), 21.67 (AcNH^{terminal}), 18.65 (T(3)$^{\gamma}$), 18.70 (T(16)$^{\gamma}$), 18.42 (V(10)$^{\gamma a}$), 18.27 (T(11)$^{*\gamma}$), 17.67 (V(10)$^{\gamma b}$), 16.28 (A(7)$^{\beta}$), 15.21 (A(4)$^{\beta}$), 15.13 (A(19)$^{\beta}$), 14.96 (A(13)$^{\beta}$); $^{\#}$: signals overlapped; MALDI-TOF-MS (DHB, positive): *m*/*z*: calcd for $C_{107}H_{169}N_{27}O_{47}$: 2584.17, found: 2585.5 $[M]^+$, 2607.1 $[M+Na]^+$, 2629.1 $[M+2Na-H]^+$.

Structural analysis—Material and methods

Structural NMR spectra

NMR spectra were recorded on Bruker 400 and 600 Avance spectrometers. All spectra were recorded in H_2O/D_2O 9:1, pH 6.5 at 298 K with peptide concentrations of 10 mM. The assignments were carried out with the help of standard DQF-COSY, TOCSY, ROESY, ^{13}C-HSQC, ^{15}N-HSQC and ^{13}C-HMBC experiments. Typically 2k data points in *F*2 and 512 experiments in *F*1 were acquired. The spectra were acquired with 16 transients and a relaxation delay of 2 s except the ROESY experiments with 80 transients. For ROESY experiments, a spinlock field of 2.8 kHz was used with a mixing time of 300 ms. The TOCSY experiments were performed with a spinlock field of 4.5 kHz using the MLEV17 sequence with mixing times of 40 ms and 80 ms. The data were zero filled and processed as 4k×1k matrix. PE COSY experiments were processed as 8k×2k matrix. To obtain the temperature coefficients of the amide proton chemical shifts, TOCSY spectra were recorded between +15 and +45 °C. The H_N–H_α coupling constants were determined by the 1D proton and DQF-COSY, PE COSY spectra.

Molecular dynamics

All molecular mechanics/dynamics simulations were performed with DISCOVER of the InsightII package (Accelrys) on a Silicon Graphics Octane workstation.[53] The simulations were done using the consistent valence force field (CVFF) that proved to account for solution NMR data to a satisfactory extent.[54] A dielectric constant (ε = 78) was used. The molecular structures were first minimized with a gradient criterion of less than 0.01 kcal mol^{-1}. The energy-minimized structures were then used for MD runs. Pseudo-atoms were used for a number of methylene proton pairs. Distance restraints derived from ROE-cross peaks, classified empirically as strong, medium, weak and very weak, were applied as biharmonic restraints with lower and upper bounds of 0.20–0.25 Å, 0.20–0.35 Å, 0.20–0.4 Å and 0.20–0.5 Å, respectively. Likewise, due to the detected *trans* configuration of all peptide bonds, the ω dihedral angle was restrained to 180°. According to a simulated annealing approach, the resulting starting molecules were heated to 600 K initially, subsequently cooled and finally, after MD at 300 K, subjected to an energy minimization using both steepest descent and conjugate gradient methods successively. Fifty structures were sampled. Eight structures within energy intervals of 15 kcal mol^{-1} and with maximum violation of upper limits less than 0.5 Å were selected. The tightness of this family of conformers was characterized by the mean pairwise RMSD for the heavy atoms or backbone atoms of the conformers and the corresponding average structure of the structural family.

Acknowledgements

This work was supported by the Deutsche Forschungsgemeinschaft (SFB-416, Project ZS and Ku 394-18) and by the Stiftung Rheinland-Pfalz für Innovation. S.D. is grateful for a doctoral fellowship provided by the Fonds der Chemischen Industrie and the Bundesministerium für Bildung und Forschung (BMBF).

[1] J. N. Blattman, P. D. Greenberg, *Science* **2004**, *305*, 200–205.
[2] P. Moingeon, *Vaccine* **2001**, *19*, 1305–1326.
[3] S. J. Danishefsky, J. A. Allen, *Angew. Chem.* **2000**, *112*, 882–911; *Angew. Chem. Int. Ed.* **2000**, *39*, 836–863.
[4] J. Taylor-Papadimitriou, J. M. Burchell, D. W. Miles, M. Dalziel, *Biochim. Biophys. Acta* **1999**, *1455*, 301–313.
[5] J. Taylor-Papadimitriou, J. M. Burchell, T. Plunkett, R. Graham, I. Correra, D. Miles, M. Smith, *J. Mammary Gland Biol. Neoplasia* **2002**, *7*, 209–221.
[6] A. M. Vlad, J. C. Kettel, N. M. Alajez, C. A. Carlos, O. J. Finn, *Adv. Immunol.* **2004**, *82*, 249–293.
[7] J. M. Burchell, A. Mungul, J. Taylor-Papadimitriou, *J. Mammary Gland Biol. Neoplasia* **2001**, *6*, 355–364.
[8] M. J. Scanlon, S. D. Morley, D. E. Jackson, M. R. Price, S. J. B. Tendler, *Biochem. J.* **1992**, *284*, 137–144.
[9] J. M. Burchell, S. J. Gendler, J. Taylor-Papadimitriou, A. Girling, A. Lewis, R. Millis, D. Lamport, *Cancer Res.* **1987**, *47*, 5476–5482.
[10] S. Dziadek, A. Hobel, E. Schmitt, H. Kunz, *Angew. Chem.* **2005**, *117*, 7803–7808; *Angew. Chem. Int. Ed.* **2005**, *44*, 7630–7635.
[11] S. Dziadek, C. Brocke, H. Kunz, *Chem. Eur. J.* **2004**, *10*, 4150–4162.
[12] B. Liebe, H. Kunz, *Angew. Chem.* **1997**, *109*, 629–631; *Angew. Chem. Int. Ed. Engl* **1997**, *36*, 618–621.
[13] B. Liebe, H. Kunz, *Helv. Chim. Acta* **1997**, *80*, 1473–1482.
[14] M. Lergenmüller, Y. Ito, T. Ogawa, *Tetrahedron* **1998**, *54*, 1381–1394.
[15] B. Helferich, F. Wedemeyer, *Liebigs Ann. Chem.* **1949**, *563*, 139–145.
[16] A. Marra, P. Sinaÿ, *Carbohydr. Res.* **1990**, *195*, 303–308.
[17] S. Keil, C. Claus, W. Dippold, H. Kunz, *Angew. Chem.* **2001**, *113*, 379–382; *Angew. Chem. Int. Ed.* **2001**, *40*, 366–369.
[18] F. Dasgupta, P. J. Garegg, *Carbohydr. Res.* **1988**, *177*, c13-c17.
[19] A. Hasegawa, H. Ohki, T. Nagahama, H. Ishida, M. Kiso, *Carbohydr. Res.* **1991**, *212*, 277–281.
[20] L. A. Carpino, G. Y. Han, *J. Am. Chem. Soc.* **1970**, *92*, 5748–5749.
[21] E. Bayer, W. Rapp, *Chem. Pept. Proteins* **1986**, *3*, 3–8; all peptide syntheses were carried out in a Perkin–Elmer ABI A 433 peptide synthesizer (Applied Biosystems).
[22] V. Dourtoglou, B. Gross, V. Lambropoulou, C. Zioudrou, *Synthesis* **1984**, 572.
[23] W. König, R. Geiger, *Chem. Ber.* **1970**, *103*, 788–798.
[24] L. A. Carpino, D. Ionescu, A. El-Faham, *J. Org. Chem.* **1996**, *61*, 2460.
[25] G. Zemplén, A. Kunz, *Chem. Ber.* **1923**, *56*, 1705–1710.

[26] P. Braun, G. M. Davies, M. R. Price, P. M. Williams, S. J. B. Tendler, H. Kunz, *Bioorg. Med. Chem.* **1998**, *6*, 1531–1545.
[27] M. Leuck, H. Kunz, *J. Prakt. Chem.* **1997**, *339*, 322–334.
[28] J. Schuman, A. P. Campbell, R. R. Koganty, B. M. Longenecker, *J. Pept. Res.* **2003**, *61*, 91–108.
[29] M. Liu, B. Acres, J.-M. Balloul, N. Bizouarne, S. Paul, P. Slos, P. Squiban, *Proc. Natl. Acad. Sci. USA* **2004**, *101*, 14567–14571.
[30] D. M. Coltart, A. K. Royyuru, L. J. Williams, P. W. Glunz, D. Sames, S. D. Kuduk, J. G. Schwarz, X.-T. Chen, S. J. Danishefsky, D. H. Live, *J. Am. Chem. Soc.* **2002**, *124*, 9833–9844.
[31] S. Mensdorff-Pouilly, L. Kirnarsky, K. Engelmann, S. E. Baldus, R. H. Verheijen, M. A. Hollingsworth, V. Pisarev, S. Sherman, F.-G. Hanisch, *Glycobiology* **2005**, *15*, 735–746.
[32] L. Kirnarsky, O. Prakash, S. M. Vogen, M. Nomoto, M. A. Hollingsworth, S. Sherman, *Biochemistry* **2000**, *39*, 12076–12082.
[33] L. Kirnarsky, M. Nomoto, Y. Ikematsu, H. Hassan, E. P. Bennett, R. L. Cerny, H. Clausen, M. A. Hollingsworth, S. Sherman, *Biochemistry* **1998**, *37*, 12811–12817.
[34] Reference [114] in S. Dziadek, C. G. Espinola, H. Kunz, *Aust. J. Chem.* **2003**, *56*, 519–543.
[35] D. S. Wishart, D. A. Case, *Methods Enzymol.* **2001**, 338, 3–34.
[36] D. E. Dorman, F. A. Bovey, *J. Org. Chem.* **1973**, *38*, 2379–2383.
[37] N. G. Delaney, V. Madison, *J. Am. Chem. Soc.* **1982**, *104*, 6635–6641.
[38] J. S. Grinstead, R. R. Koganty, M. J. Krantz, B. M. Longenecker, A. P. Campbell, *Biochemistry* **2002**, *41*, 9946–9961.
[39] D. S. Wishart, B. D. Sykes, F. M. Richards, *J. Mol. Biol.* **1991**, *222*, 311–333.
[40] N. H. Andersen, J. W. Neidigh, S. M. Harris, G. M. Lee, Z. Liu, H. Tong, *J. Am. Chem. Soc.* **1997**, *119*, 8547–8561.
[41] G. D. Rose, L. M. Gierasch, J. A. Smith, *Adv. Protein Chem.* **1985**, *37*, 1–109.
[42] H. J. Dyson, P. E. Wright, *Annu. Rev. Phys. Chem.* **1996**, *47*, 369–395.
[43] D. H. Live, L. J. Williams, S. D. Kuduk, J. B. Schwarz, D. W. Glunz, X.-T. Chen, D. Sames, R. A. Kumar, S. J. Danishefsky, *Proc. Natl. Acad. Sci. USA* **1999**, *96*, 3489–3493.
[44] G. A. Naganagowda, T. L. Gururaja, J. Satyanarayana, M. J. Levine, *J. Pept. Res.* **1999**, *54*, 290–310.
[45] D. Pal, P. Chakrabarti, *Acta Crystallogr. Sect. D* **2000**, *56*, 589–594.
[46] J. Schuman, D. Qiu, R. R. Koganty, B. M. Longenecker, A. P. Campbell, *Glycoconjugate J.* **2000**, *17*, 835–848.
[47] L. Kirnarsky, G. Suryanarayanan, O. Prakash, H. Paulsen, H. Clausen, F.-G. Hanisch, M. A. Hollingsworth, S. Sherman, *Glycobiology* **2003**, *13*, 929–939.
[48] J. S. Grinstead, J. T. Schuman, A. P. Campbell, *Biochemistry* **2003**, *42*, 14293–14305.
[49] H. Takeuchi, K. Kato, K. Denda-Nagai, F.-G. Hanisch, H. Clausen, T. Irimura, *J. Immunol. Methods* **2002**, *270*, 199–209.
[50] J. D. Fontenot, S. V. Mariappan, P. Catasti, N. Domenech, O. J. Finn, G. Gupta, *J. Biomol. Struct. Dyn.* **1995**, *13*, 245–260.
[51] D. D. Perrin, W. L. F. Armarego, *Purification of Laboratory Chemicals*, Pergamon Press, Oxford, 3 ed., **1988**.
[52] L. A. Carpino, H. Imazumi, A. El-Faham, F. J. Ferrer, C. Zhang, Y. Lee, B. M. Foxmann, P. Henklein, C. Hanay, C. Mügge, H. Wenschuh, J. Klose, M. Beyermann, M. Bienert, *Angew. Chem.* **2002**, *114*, 457–461; *Angew. Chem. Int. Ed.* **2002**, *41*, 441–445.
[53] P. Dauber-Osguthorpe, V. A. Roberts, D. J. Osguthorpe, J. Wolff, M. Genest, A. T. Hagler, *Proteins Struct. Funct. Genet.* **1988**, *4*, 31–47.
[54] M. Martín-Pastor, J. F. Espinosa, J. L. Asensio, J. Jiménez-Barbero, *Carbohydr. Res.* **1997**, *298*, 15–49.

Received: February 2, 2006
Published online: April 27, 2006

